A NEW APPROACH TO VISION AND CONTROL FOR ROAD FOLLOWING

Daniel Raviv

Florida Atlantic University
The Robotics Center and
The Electrical Engineering Department
Boca Raton, FL 33431

and

Martin Herman

U.S. DEPARTMENT OF COMMERCE
National Institute of Standards
and Technology
Robot Systems Division
Bldg. 220 Rm. B124
Gaithersburg, MD 20899

NIST

A NEW APPROACH TO VISION AND CONTROL FOR ROAD FOLLOWING

Daniel Raviv

Florida Atlantic University
The Robotics Center and
The Electrical Engineering Department
Boca Raton, FL 33431

and

Martin Herman

U.S. DEPARTMENT OF COMMERCE
National Institute of Standards
and Technology
Robot Systems Division
Bldg. 220 Rm. B124
Gaithersburg, MD 20899

A NEW APPROACH TO VISION AND CONTROL FOR ROAD FOLLOWING

Daniel Raviv* and Martin Herman**

*Robotics Center and Electrical Engineering Department
Florida Atlantic University, Boca Raton, FL 33431; and
Sensory Intelligence Group, Robot Systems Division
National Institute of Standards and Technology (NIST)
Bldg 220, Room B124, Gaithersburg, MD 20899

**Sensory Intelligence Group, Robot Systems Division
National Institute of Standards and Technology (NIST)
Bldg 220, Room B124, Gaithersburg, MD 20899

1

ABSTRACT

This paper deals with a new quantitative, vision-based approach to road following. It is based on the theoretical framework of the recently developed optical flow-based visual field theory. By building on this theory, we suggest that motion commands can be generated directly from a visual feature, or cue, consisting of the projection into the image of the tangent point to the edge of the road, along with the optical flow of this point. Using this cue, we suggest several different vision-based control approaches. There are several advantages to using this visual cue: (1) it is extracted directly from the image, i.e., there is no need to reconstruct the scene, (2) for many road following situations this is the only necessary visual cue, (3) only the horizontal component of the optical flow of the tangent point needs to be extracted, (4) it has a scientific basis, i.e., the described techniques are not *ad hoc*, (5) the related computations are relatively simple and thus suitable for real-time applications. For each control approach, we derive the value of the related steering commands.

1. INTRODUCTION

Autonomous visually-guided road following by a ground vehicle requires two basic steps. The first step is to extract relevant road features from images taken by on-board cameras. This step involves finding road regions, road edges and boundaries, center lines, highway lane lines, etc. in complex real-world images. The second step is to determine how to steer the vehicle (as well as how to speed up or slow down) once visual road information has been extracted. Algorithms for both steps have recently been explored by many investigators [2, 3, 4, 9, 10, 11]. Most of these investigators, however, have approached these problems using *ad hoc* techniques. That is, the determination of which road features to extract, as well as how to use them to make steering decisions, has been done in an *ad hoc* manner.

This paper approaches the road following problem by building on the theoretical framework of the recently developed visual field theory [7, 8]. This theory provides quantitative relationships between a stationary 3-D environment and a moving camera. The theory involves pre-computing the expected instantaneous optical flow values in the camera imagery arising from every point in 3-D space. The theory provides a theoretical and scientific basis for optical flow-based road following algorithms.

This paper is concerned with an analysis of the road following problem. Using the visual field theory, we develop geometric and motion-related relationships and constraints for road following. These then suggest partial control algorithms as well as visual cues that can serve as input signals to control algorithms. Rather than suggesting that one control approach is superior to another, the paper details many different control options. Any one of these, or some combination, can be used in the development of the actual control algorithms. The control schemes presented are partial since only the kinematics of the vehicle and the camera are considered. Also, stability, robustness and sensitivity issues are not considered in this paper. Some of the visual cues suggested in this paper have been used to develop road following control algorithms for a real mobile robot [12]. Further experiments are planned in the future to validate the control schemes presented here.

This paper has suggestions for algorithms for both steps described above. For the first step, involving the extraction of road features, this paper suggests that the only road feature necessary (for curved, convex roads) is the tangent point on the road edge (i.e., the point on the road edge lying on an imaginary line tangent to the road edge and passing through the camera) and its optical flow. Therefore, all image processing effort should be directed towards reliably finding and tracking the tangent point and extracting its optical flow. This is in contrast to most current systems which attempt to find as much about the road as possible. Existing systems often ignore the tangent point when making steering decisions, and usually are not concerned with the optical flow values of points on the road.

For the second step that involves determining steering commands once visual information has been extracted, this paper suggests that fast, computationally inexpensive, and simple control algorithms can be used. Given the desired distance from the

3

edge of the road, the only visual information these algorithms would require is the location of the tangent point (in the image) and its optical flow. Other inputs to these algorithms would be the current steering angle, the current vehicle speed, etc. The output of these control algorithms is the change in steering angle for the next instant of time. (In this paper, we do not consider decisions about speed and acceleration of the vehicle.) Most existing road following algorithms convert the information extracted from images into a 3-D, vehicle-centered cartesian coordinate system aligned with the ground plane. Steering decisions are then determined in this coordinate system. A 3-D reconstruction is therefore performed before steering decisions are made. We suggest that control algorithms can be developed which directly use image information represented in the 2-D image coordinate system (e.g., image position and image flow). There are two main advantages to such approaches. The first is that since 3-D reconstruction results in inferred quantities (i.e., recovering the third dimension), control that is based on this method is not as robust as control based on directly observable 2-D image quantities [1]. Second, control based on 2-D image quantities is simpler and requires much less computation; it is therefore much faster.

This paper begins by outlining our assumptions and defining road following, the coordinate system, and the vehicle. We then review the visual field theory as it relates to road following. Next, we provide analyses and suggest partial control schemes for two road following scenarios, one for circular roads and the other for curved roads. Finally, we discuss directions for future work.

2. DEFINITIONS AND ASSUMPTIONS

2.1. ROAD FOLLOWING

We define a *road* as any continuous, extended, curvilinear feature. The goal of road following is to follow along this feature over an extended period of time. In what we normally think of as road following, a road is defined either by its boundaries or by an extended solid or dashed white line. Here, the goal is not only to follow along these features but also to stay within a constant lateral distance from these features. In general, the feature to be followed need not define a real road. For example, it could be a boundary line of vegetation, a stripe painted on the ground, or even a wall. For a low-flying air vehicle, the feature to be followed could be a river.

Vision-based road following requires the ability to continuously detect and track features in imagery obtained from an onboard camera, and to make steering decisions based on visual properties of these features.

Figure 1 shows a vehicle on a road and the left-hand side road edge. The unit vector $\hat{h}$ is the instantaneous heading of the vehicle, O is the instantaneous center of curvature of the vehicle path, and r is the instantaneous radius of curvature of this path. We define *road following* as an activity that involves servoing $\hat{h}$ such that it follows the road edge. It is desired that $\hat{h}$ be servoed such that the vehicle is always parallel to the tangent to the local curvature of the road edge (Figure 1b), and such that the distance s

of a point on the vehicle from the road edge is maintained at a constant value. In other words, the instantaneous center of curvature of the road edge and the instantaneous center of curvature of the vehicle path should coincide, and the tangent to the edge of the road at the intersection point B should be parallel to $\hat{h}$. Normally, these constraints will not be met if the vehicle is attempting to avoid an obstacle or if the vehicle is changing lanes on a road. If a road has two boundaries, then road following will normally involve staying within these boundary edges. In this paper, we assume that the road is always curved and we do not discuss the two-boundary case.

2.2. COORDINATE SYSTEM

The equations in this paper will be defined in a coordinate system which is fixed with respect to the camera on board the vehicle. This coordinate system is shown in Figure 2. We assume that the camera is mounted on a vehicle (later we explain how) moving in a stationary environment. Assume a pinhole camera model and that the pinhole point of the camera is at the origin of the coordinate system. This coordinate system is used to measure angles to points in space and to measure optical flow at these points. We use spherical coordinates $(R-\theta-\phi)$ for this purpose. In this system, angular velocities ($\dot{\theta}$ and $\dot{\phi}$) of any point in space, say P, are identical to the optical flow values at P' in the image domain. Figure 3 illustrates this concept: θ and ϕ of a point in space are the same as θ and ϕ of the projected point P' in the image domain, and therefore there is no need to convert angular velocities of points in 3D space to optical flow. In Figure 3 the image domain is a sphere. However, for practical purposes the surface of the image sphere can be mapped onto an image plane (or other surface).

2.3. TWO-WHEELED VEHICLE

For our analysis, we use a theoretical two-wheeled vehicle as illustrated in Figure 4. A rigid frame of length $2m$ holds both wheels. A steering wheel angle is applied to both wheels simultaneously, i.e., if one wheel is rotated by an angle β relative to the frame, the other wheel will rotate by the same angle. This apparatus assures that both wheels will always stay at the same distance from the instantaneous center of curvature of the vehicle's path. As shown in Figure 4, the camera is mounted such that its pinhole point is located above the front wheel center, and it rotates with the front wheel. The optical axis of the camera coincides with the instantaneous translation vector (heading) of the front wheel. Note that the heading vector of other points on the vehicle may not be the same as the chosen one.

The following geometrical relationship holds for the vehicle in Figure 4:

$$r = \frac{m}{\sin\beta} \tag{1}$$

The frame length m is usually known. Thus the instantaneous radius of curvature r of the vehicle path can be determined by measuring the steering angle β.

Figure 5 is an overall description of the system including the spherical coordinate system, and Figure 6 is the related top view. For convenience we chose to have the Z axis pointing down. However the same coordinate system as described in Figure 2 is used here. The camera is mounted at some height above the ground and rotates with the front wheel. The position of any point on the road can be expressed with the coordinates R, θ and ϕ, as shown in Figure 5.

In the following analysis, we assume a moving vehicle in a stationary environment. The road is assumed to be planar, and road edges are assumed to be extractable. Figure 7 is an example of a road image obtained from a camera mounted on a vehicle.

3. VISUAL FIELD THEORY

We have recently developed a new visual field theory that relates six-degree-of-freedom camera motion to optical flow for a stationary environment [7, 8]. The theory describes the structure of a field in 3-D space consisting of contours and surfaces surrounding the moving camera. If static objects are placed anywhere in the surrounding space, the optical flow produced by these objects in the camera is predicted by the field theory. The field is always centered at the camera pinhole point and moves with the camera. The structure of the field changes as a function of the instantaneous camera motion.

This theory provides us with a theoretical and scientific basis for developing constraints, control schemes, and optical flow-based visual cues for road following. This section reviews this theory as it relates to the road following problem.

3.1. EQUATIONS OF MOTION AND OPTICAL FLOW

First we describe the equations that relate a point in 3-D space to the projection of that point in the image for general six-degree-of-freedom motion of the camera. Some of the equations can be found in many books, e.g., see [5].

We start with the derivation of the velocity of a 3-D point in the XYZ coordinates (Figure 2). Let the instantaneous coordinates of the point P be $\mathbf{R} = (X, Y, Z)^T$ (where the superscript T denotes transpose). If the instantaneous translational velocity of the camera is $\mathbf{t} = (U, V, W)^T$ and the instantaneous angular velocity is $\omega = (A, B, C)^T$ then the velocity vector $\mathbf{V}$ of the point P with respect to the XYZ coordinate system is:

$$\mathbf{V} = -\mathbf{t} - \omega \times \mathbf{R} \tag{2}$$

or:

$$V_X = -U - BZ + CY \tag{3}$$

$$V_Y = -V - CX + AZ \tag{4}$$

$$V_Z = -W - AY + BX \tag{5}$$

where V_X, V_Y, and V_Z are the components of the velocity vector $\mathbf{V}$ along the X, Y, and Z directions respectively.

6

To convert from $R\theta\phi$ to XYZ coordinates we use the relations:

$$X = R\cos\phi\cos\theta \tag{6}$$

$$Y = R\cos\phi\sin\theta \tag{7}$$

$$Z = R\sin\phi. \tag{8}$$

Similarily, to convert from XYZ to $R\theta\phi$ coordinates we use:

$$R = \sqrt{X^2+Y^2+Z^2} \tag{9}$$

$$\theta = \tan^{-1}\frac{Y}{X} \tag{10}$$

$$\phi = \sin^{-1}\frac{Z}{\sqrt{X^2+Y^2+Z^2}}. \tag{11}$$

In order to find the optical flow of a 3-D point in $R\theta\phi$ coordinates, we use the following relations and transformations (see [6] and Figure 2):

Let V_R, V_θ, and V_ϕ be the components of the vector $\mathbf{V}$ in spherical coordinates, and

$$V_{R\theta\phi} = \begin{bmatrix} V_R \\ V_\theta \\ V_\phi \end{bmatrix} \tag{12}$$

$$V_{XYZ} = \begin{bmatrix} V_X \\ V_Y \\ V_Z \end{bmatrix}. \tag{13}$$

Then:

$$V_{R\theta\phi} = [T_\phi][T_\theta]V_{XYZ} \tag{14}$$

where

$$[T_\theta] = \begin{bmatrix} \cos\theta & \sin\theta & 0 \\ -\sin\theta & \cos\theta & 0 \\ 0 & 0 & 1 \end{bmatrix} = \begin{bmatrix} \dfrac{X}{\sqrt{X^2+Y^2}} & \dfrac{Y}{\sqrt{X^2+Y^2}} & 0 \\ \dfrac{-Y}{\sqrt{X^2+Y^2}} & \dfrac{X}{\sqrt{X^2+Y^2}} & 0 \\ 0 & 0 & 1 \end{bmatrix} \tag{15}$$

and

$$[T_\phi] = \begin{bmatrix} \cos\phi & 0 & \sin\phi \\ 0 & 1 & 0 \\ -\sin\phi & 0 & \cos\phi \end{bmatrix} = \begin{bmatrix} \dfrac{\sqrt{X^2+Y^2}}{\sqrt{X^2+Y^2+Z^2}} & 0 & \dfrac{Z}{\sqrt{X^2+Y^2+Z^2}} \\ 0 & 1 & 0 \\ \dfrac{-Z}{\sqrt{X^2+Y^2+Z^2}} & 0 & \dfrac{\sqrt{X^2+Y^2}}{\sqrt{X^2+Y^2+Z^2}} \end{bmatrix}. \tag{16}$$

Also (see [6]):

$$V_R = \dot{R} \tag{17}$$

$$V_\theta = R\,\dot{\theta}\,\cos\phi \tag{18}$$

$$V_\phi = R\,\dot{\phi} \tag{19}$$

where dot denotes first derivative with respect to time.

Using equations (3)-(19) yields the following expressions:

$$\begin{bmatrix} R\,\dot{\theta}\,\cos\phi \\ R\,\dot{\phi} \end{bmatrix} = \begin{bmatrix} -\sin\theta & \cos\theta & 0 \\ -\sin\phi\cos\theta & -\sin\phi\sin\theta & \cos\phi \end{bmatrix} \begin{bmatrix} -U-BZ+CY \\ -V-CX+AZ \\ -W-AY+BX \end{bmatrix} \tag{20}$$

or

$$\begin{bmatrix} \dot{\theta} \\ \dot{\phi} \end{bmatrix} = \begin{bmatrix} \dfrac{-Y}{X^2+Y^2} & \dfrac{X}{X^2+Y^2} & 0 \\[2ex] \dfrac{-XZ}{\sqrt{X^2+Y^2}(X^2+Y^2+Z^2)} & \dfrac{-YZ}{\sqrt{X^2+Y^2}(X^2+Y^2+Z^2)} & \dfrac{\sqrt{X^2+Y^2}}{X^2+Y^2+Z^2} \end{bmatrix} \begin{bmatrix} -U-BZ+CY \\ -V-CX+AZ \\ -W-AY+BX \end{bmatrix}. \tag{21}$$

As mentioned earlier, $\dot{\theta}$ and $\dot{\phi}$ of a point in space (i.e., the angular velocities in the camera coordinate system) are the *same* as the optical flow components $\dot{\theta}$ and $\dot{\phi}$ (Figure 3).

Suppose that we want to determine the locus of points in 3D space that produce constant optical flow values $\dot{\theta}$ and constant optical flow values $\dot{\phi}$ in the image for a given arbitrary six-degree-of-freedom camera motion. To do so we simply set $\dot{\theta}$ and $\dot{\phi}$ in equation set (21) to the desired constants and solve for X, Y, and Z. All points in 3-D space that satisfy this solution are called *equal flow points*. However, the solution to these two equations is not unique since there are three unknowns and two equations. In general, there is an infinite number of solutions.

3.2. A SPECIAL CASE

In this section we analyze a specific motion in the instantaneous XY ($\phi = 0$) plane of the camera coordinate system.

Let the camera motion vectors t and ω be given as follows:

$$\mathbf{t} = (U,V,0)^T \tag{22}$$

$$\boldsymbol{\omega} = (0,0,C)^T. \tag{23}$$

This means that the translation vector may lie anywhere in the instantanous XY plane while the rotation is about the Z-axis. Substituting these motion vectors into equation set (21) yields:

$$\begin{bmatrix} \dot{\theta} \\ \dot{\phi} \end{bmatrix} = \begin{bmatrix} \dfrac{-Y}{X^2+Y^2} & \dfrac{X}{X^2+Y^2} & 0 \\[2ex] \dfrac{-XZ}{\sqrt{X^2+Y^2}(X^2+Y^2+Z^2)} & \dfrac{-YZ}{\sqrt{X^2+Y^2}(X^2+Y^2+Z^2)} & \dfrac{\sqrt{X^2+Y^2}}{X^2+Y^2+Z^2} \end{bmatrix} \begin{bmatrix} -U+CY \\ -V-CX \\ 0 \end{bmatrix} \tag{24}$$

8

Setting $\dot{\theta}$ and $\dot{\phi}$ in equation set (24) to constants will result in a set of equal flow points for this specific motion.

Consider the case where the optical flow value of $\dot{\theta}$ is constant. From equation set (24), the points in space that result from constant $\dot{\theta}$ (regardless of the value of $\dot{\phi}$) form a cylinder of infinite height whose equation is

$$\left[X+\frac{V}{2(C+\dot{\theta})}\right]^2+\left[Y-\frac{U}{2(C+\dot{\theta})}\right]^2=\left[\frac{V}{2(C+\dot{\theta})}\right]^2+\left[\frac{U}{2(C+\dot{\theta})}\right]^2, \tag{25}$$

as displayed in Figure 8.

Figure 9 shows a horizontal section of the cylinder of Equation (25). The section is a circle that lies in the XY plane. This plane is perpendicular to the axis of symmetry of the cylinder. The radius of the circle is $\left[\left[\frac{V}{2(C+\dot{\theta})}\right]^2+\left[\frac{U}{2(C+\dot{\theta})}\right]^2\right]^{\frac{1}{2}}$ and its center is at $\left[-\frac{V}{2(C+\dot{\theta})}, \frac{U}{2(C+\dot{\theta})}\right]$. The circle is tangent to the camera translation vector at the origin.

The meaning of equation (25) is the following: all points in 3-D space that lie on the cylinder described by Equation (25) and which are visible (i.e., unoccluded and in the field of view of the camera) produce the same instantaneous horizontal optical flow $\dot{\theta}$. We call the cylinder on which equal flow points lie the *equal flow cylinder*. A section of a set of equal flow cylinders is illustrated in Figure 10 for the case where the camera undergoes instantaneous translation and rotation. The label of each circle represents the horizontal optical flow $\dot{\theta}$ in the image that corresponds to points on this circle. Here, there is a circle with finite radius that produces zero horizontal flow ($\dot{\theta} = 0$ in the image domain).

3.3. ZERO FLOW CYLINDERS

One of the equal flow cylinders corresponds to points in 3-D space that produce zero horizontal flow. We call this cylinder a *zero flow cylinder*. The equation that describes the zero flow cylinder can be obtained by setting $\dot{\theta} = 0$ in Equation (25), i.e.,

$$\left[X+\frac{V}{2C}\right]^2+\left[Y-\frac{U}{2C}\right]^2=\left[\frac{V}{2C}\right]^2+\left[\frac{U}{2C}\right]^2. \tag{26}$$

We have shown [7] that if the Z component of the camera rotation vector ω is positive (i.e., $C > 0$), then visible points in the XY plane that are inside the zero flow cylinder produce positive horizontal optical flow ($\dot{\theta} > 0$), while visible points outside the zero flow cylinder produce negative horizontal optical flow ($\dot{\theta} < 0$) in the image (see Figure 11). If ω is negative (i.e., $C > 0$) then the opposite is true.

3.4. EQUAL FLOW CYLINDERS AS A FUNCTION OF TIME

As the camera moves through 3-D space, the equal flow cylinders move with it. Figure 12 shows sections of equal flow cylinders as a function of time. At each instant of time, the radii of the equal flow cylinders are a function of the instantaneous motion parameters t and ω. The locations of the equal flow cylinders are such that they always contain the origin of the camera coordinate system (the same as the camera pinhole point), are tangent to the instantaneous translation vector t, and their symmetry axes are parallel to the instantaneous rotation vector ω. (In Figure 12, the direction of ω varies over time.) Each zero flow cylinder lies to the left or right of the translation vector depending on whether the instantanous rotation is positive or negative, respectively.

4. ANALYSIS OF ROAD FOLLOWING

We describe two road following scenarios. The first one is for a circular road, where we outline basic geometric and motion-related relationships. Using this relatively simple case, we explain the problem of following a road using a vision sensor, problems associated with it, and relate it to the visual field theory described above. We also suggest several road following control approaches. The second road following scenario is for an arbitrary convex curved road, where we also suggest some control approaches.

4.1 CIRCULAR ROAD

In this section, we consider following along a circular road. Given visual cues, a goal of a control system is to find the steering angle. If the vehicle is already on a path that follows the road, then only *changes* in steering angle are necessary. Figure 13 shows a vehicle moving around a circular road of radius l. The path traversed by the vehicle is a circle of radius r. Let the unit vector $\hat{i}$ indicate the direction of the *tangent line,* a line that contains the camera pinhole point and is tangent to the road edge.

We will show next that the tangent point T lies on the instantaneous zero flow cylinder if the camera orientation is fixed relative to the vehicle. The proof for this is as follows. Let us consider the planar case first, as shown in Figure 13. Given that the line AT is tangent to the road edge, then AT is perpendicular to OT. We will now show that OA is the diameter of the section of the zero flow cylinder displayed in Figure 13. From Equation 25, we can see that the center of the zero flow cylinder section is at $\left[-\dfrac{V}{2(C+\dot{\theta})} , \dfrac{U}{2(C+\dot{\theta})} \right]$ (Figure 9). Further, the location of the camera is at (0,0). Now the center of rotation of the camera's circular path must lie on the zero flow cylinder section. To see why, we first note that the vector from the camera to the center of rotation O is always perpendicular to the camera heading vector. (Remember that the heading vector and camera optical axis coincide.) Therefore the center O can be considered as a fixation point for the camera during its motion, i.e., the position of point O does not change relative to the camera's coordinate system [7, 8]. This means that this point must theoretically produce zero horizontal optical flow in the camera (assuming the

camera has a wrap-around lens). Therefore, point O must lie on the zero flow cylinder section. Then the center of rotation of the camera's circular path must be at $\left[-\dfrac{V}{(C+\dot{\theta})} , \dfrac{U}{(C+\dot{\theta})} \right]$ (Figure 9). Therefore line OA is the diameter of the zero flow cylinder. Since the angle OTA is a right angle, point T must lie on the circle whose diameter is OA. Since this circle is a section of the zero flow cylinder, point T must lie on this cylinder. For the case where the road edge does not lie in the $X-Y$ plane of the camera, all points above or below the point T (including the one on the edge of the road) lie on the zero flow cylinder.

Notice that this proof holds no matter what the diameter of the circular road edge. This means that no matter how far the vehicle is from the road edge (Figure 14), the tangent point lies on the zero flow cylinder. Thus the horizontal component of optical flow of the tangent point is always zero.

In Figure 13, therefore, the optical flow $\dot{\theta}$ due to point T is zero. Let the distance from the vehicle to the road edge be s, and let θ be the positive angle to $\dot{r}$ measured from the X-axis. From Figure 13, the following relationships hold:

$$l = r \sin\theta \tag{27}$$

$$s = r - l = r(1 - \sin\theta) \tag{28}$$

Differentiating Equation (27) with respect to time:

$$\dot{l} = \dot{r}\sin\theta + r\dot{\theta}\cos\theta \tag{29}$$

where dot denotes derivative with respect to time. For a circular road, l is constant, and thus $\dot{l}$ can be set to zero in Equation (29):

$$0 = \dot{r}\sin\theta + r\dot{\theta}\cos\theta$$

$$\dot{r} = -r\,\dot{\theta}\,\cot\theta \tag{30}$$

When the vehicle is moving on a perfect circular path both $\dot{r}$ and $\dot{\theta}$ are equal to zero. However, suppose the vehicle's path is not a perfect circle. Since r is the instantaneous radius of curvature of the vehicle motion, $\dot{r}$ is the rate at which the curvature changes. Equation (30) suggests a way of controlling the vehicle motion so as to achieve a constant circular motion. Consider the two-wheeled vehicle described in Section 2.3. From Equation (1), we can derive the following:

$$\beta = \sin^{-1}\left(\frac{m}{r}\right). \tag{31}$$

Equation (31) gives a value of the steering angle β as a function of the instantaneous radius of curvature r and the distance $2m$ between the two wheels. Normally the value m is known. For a more realistic vehicle (e.g., Figure 15), some other relationship may hold.

In Equation (30), $\dot{r}$ is the rate at which the radius of curvature of the vehicle motion is changing. We can express $\dot{r}$ as a function of the steering angle β by

differentiating Equation (1) with respect to time:

$$\dot{r} = \frac{-m \cos\beta}{\sin^2\beta}\,\dot{\beta} \qquad (32)$$

Substituting Equations (32) and (1) into (30) and solving for $\dot{\beta}$:

$$\dot{\beta} = \dot{\theta}\,\tan\beta\,\cot\theta \qquad (33)$$

Equation (33) suggests a partial control scheme whose inputs are the current steering angle β, the current angle θ of the tangent line relative to the X-axis, and the optical flow $\dot{\theta}$ of the tangent point. All of these inputs can be measured. The variable being computed is the rate of change of the steering angle, $\dot{\beta}$. Equation (33) provides the gain $\tan\beta \cot\theta$ by which $\dot{\theta}$ should be multiplied in order to get the correct change in steering wheel angle. This gain depends on the current steering wheel angle β and the angular location θ of the tangent point in the image. Note that Equations (1) and (31) hold only for certain types of vehicles. Vehicles with other wheel and steering configurations (e.g., Figure 15) will result in different expressions relating steering angle to the radius of curvature of motion. In all such expressions, however, there should be a one-to-one relationship between β and r. These expressions can then be substituted into Equation (30) to derive the relevant control signals. It is important to emphasize that the derivation of $\dot{\beta}$ takes into account the kinematics of the system but *not* the dynamics. This is also the reason why we emphasize that the control scheme is not complete.

If the rate of change of the steering angle, $\dot{\beta}$, is the only variable being controlled (as indicated in Equation (33)), then in practice the vehicle may not maintain a constant distance from the edge of the road. Therefore, in addition to Equation (33), Equation (28) can also be used to control the vehicle to achieve a constant circular motion. Substituting Equation (1) into (28):

$$s = \frac{m}{\sin\beta}(1-\sin\theta)$$

or

$$\beta = \sin^{-1}[\frac{m}{s}(1-\sin\theta)] \qquad (34)$$

Equation (34) suggests a partial control scheme whose inputs are the measured angle θ of the tangent line relative to the X-axis, the desired distance s of the vehicle from the road edge, and the distance $2\,m$ between the front and rear wheels. The variable being computed is the steering angle β.

The control signals (β and $\dot{\beta}$) and partial control schemes suggested above assume that the road is circular, that the center of curvature of the vehicle path coincides with the center of curvature of the circular road, and that the road is planar. It is also assumed that the tangent point (in the image) is traceable, and that the vehicle heading coincides with the camera optical axis. There are several advantages to this approach: (1) it is simple and therefore computationally inexpensive, (2) it is independent of the

speed of the vehicle, (3) it is independent of the camera height above the road, (4) only a few measurements are necessary to control the vehicle, and (5) only a very small portion of the image -- the portion around the tangent point -- needs to be analyzed, in principle. (Of course, item (5) may not be true in practice since larger portions of the road may have to be extracted in order to reliably find the tangent point.)

A different approach for circular road following is based on the simple fact that the height of the camera above the road is constant during driving. Refer to Figures 5 and 13. Let h_c be the height of the camera above the ground. For the tangent point T we can write:

$$h_c = r \cos\theta \tan\phi \tag{35}$$

or

$$r = \frac{h_c}{\cos\theta \tan\phi} \tag{36}$$

The value h_c is usually a known constant, while θ and ϕ for the tangent point can be measured in the image. Thus the distance r of the camera from the center of curvature of the circular road can be determined. Equations (36) and (31) allow computing the steering wheel angle β using visual information without measuring it directly.

Taking the derivative of equation (35) with respect to time yields:

$$\dot{h_c} = \dot{r} \cos\theta \tan\phi + r (-\sin\theta) \tan\phi \, \dot{\theta} + r \cos\theta \, \frac{1}{\cos^2\phi} \, \dot{\phi} \tag{37}$$

Since h_c is constant, then $\dot{h_c} = 0$ in Equation (37), and solving for $\dot{r}$:

$$\dot{r} = (\dot{\theta} \tan\theta - \frac{2\dot{\phi}}{\sin2\phi}) \, r \tag{38}$$

The corresponding change in steering angle is (using equations (32) and (38)):

$$\dot{\beta} = -\frac{1}{m} \sin\beta \tan\beta \, (\dot{\theta} \tan\theta - \frac{2\dot{\phi}}{\sin2\phi}) \, r \tag{39}$$

Substituting $\beta = \sin^{-1}(\frac{m}{r})$ (Equation (31)) and then $r = \frac{h_c}{\cos\theta\tan\phi}$ (Equation (36)) in Equation (39) results in an expression for $\dot{\beta}$ as a function of the visually measured parameters $\theta,\phi,\dot{\theta},\dot{\phi}$ and the known constants m and h_c.

Yet another approach for circular road following is depicted in Figure 16. A circular path will be maintained by the vehicle if the heading vector $\hat{h}_A$ at point A is smoothly servoed so as to result in a heading vector $\hat{h}_B$ at point B. It is desired that the heading vector always be tangent to the circular path concentric with the circular road and at a radial distance s from the road edge. Let θ be the angle between the camera X-axis and the tangent line, and let $\alpha = \frac{\pi}{2} - \theta$. Notice that since it is desired that $\hat{h}_B$ be parallel to the tangent line from point A, the change in direction between $\hat{h}_A$ and $\hat{h}_B$ is α.

13

We define the *turning rate* as the amount the heading vector direction changes (or turns) per unit time.

Since the circular arc length between points A and B is $(s + l)\,\alpha$, it takes the vehicle $\dfrac{(s + l)\,\alpha}{v}$ amount of time to travel the length of the arc, where v is the speed of the vehicle (assuming constant speed). Therefore

$$Turning\ Rate\ = \frac{\alpha}{\dfrac{(s+l)\alpha}{v}} = \frac{v}{s+l}. \tag{40}$$

For the two-wheeled vehicle in Figure 4, the turning rate is proportional to the rate of change of the steering angle, i.e., $\dot{\beta}$.

4.2 CURVED ROAD FOLLOWING

In this section, we consider road following for the case where the curvature of a convex road is not constant. Figure 17 shows two cases. In Figure 17a the radius of curvature increases as the vehicle moves. In Figure 17b, the radius of curvature decreases. Figure 18 shows a detailed version of Figure 17a. Let the current instantaneous center of curvature of the vehicle path be at O. If the road curvature were constant, then the point of tangency of the vector $\hat{\imath}$ would be at T and this point would lie on the zero flow cylinder. However, because the road's curvature is changing, the point of tangency is at T'. The center of curvature of the curve at T' is at O'. Notice that the point T' lies on some equal flow cylinder whose $\dot{\theta}$ optical flow is negative (T' lies outside the zero flow cylinder). If the radius of curvature were decreasing (Figure 17b), the tangent point would lie inside the zero flow cylinder, and its $\dot{\theta}$ optical flow would be positive. Therefore, intuitively, if the horizontal component of the optical flow, $\dot{\theta}$, at the tangent point is measured, then its value can be used as a control signal for steering the vehicle. If $\dot{\theta}$ is negative (Figure 17a) then the steering command is to increase the radius of curvature of the vehicle's current motion. If $\dot{\theta}$ is positive (Figure 17b), then the steering command is to decrease the radius of curvature of the vehicle's current motion by sharpening the turn.

Another approach to curved road following is to extend the technique shown in Figure 16. Consider Figure 19, which shows the case of a road whose radius of curvature is increasing. As before, the goal is to smoothly servo the heading vector $\hat{h}_A$ at point A so as to result in a heading vector $\hat{h}_B$ at point B. The vector $\hat{h}_B$ is parallel to the tangent line from point A and is at a distance s from the line. If $\alpha = \dfrac{\pi}{2} - \theta$ is the angle between $\hat{h}_A$ and the tangent line, then the change in direction between $\hat{h}_A$ and $\hat{h}_B$ is α. Let the distance between the vehicle and the tangent point T be a. Later we will discuss how a might be computed. The arc between points A and B can be very closely approximated by an arc of a circle. The straight line distance between A and B is $\sqrt{a^2+s^2}$. The ratio between the arc AB and the line AB is $\dfrac{\alpha}{2\sin\dfrac{\alpha}{2}}$ (assuming arc AB is a circle). Then

$$Turning \ Rate \ = \ \frac{2 \ v \ \sin(\frac{\pi}{4} - \frac{\theta}{2})}{\sqrt{a^2 + s^2}}. \tag{41}$$

A way to compute a in Equation (41) is as follows. Suppose the camera is located at a height h_c above the ground (Figure 20). The angle between the horizontal and the tangent line is ϕ. Then, from Figure 20,

$$a \ = \ \frac{h_c}{\tan\phi} \tag{42}$$

Since angle ϕ can be measured in the image and h_c is a known constant, it is easy to compute a from Equation (42).

Equation (41) gives the turning rate to achieve road following. The quantities that need to be measured to achieve this are the angle θ between the X-axis and tangent vector, the value a, and the velocity v of the vehicle. The value s is assumed to be given.

A somewhat different method of controlling the vehicle can also be derived from Figure 19. This method assumes that the control scheme is to continuously compute a desired future location for the vehicle (point B in Figure 19) relative to the vehicle's current location (point A) and to the tangent point (point T). This can be done as follows. From Figure 19:

$$s \ = \ a \ \tan\Delta\theta$$

$$\Delta\theta \ = \ \tan^{-1}\frac{s}{a} \tag{43}$$

Combining Equations (42) and (43):

$$\Delta\theta \ = \ \tan^{-1}(\frac{s}{h_c}\tan\phi) \tag{44}$$

Equation (44) gives the direction $\Delta\theta$ of the desired point B relative to the direction of the tangent point T. The control approach is then to continuously measure ϕ and servo the heading vector in the direction $\Delta\theta$. This approach has the advantage of observing a visible point (the tangent point) and servoing toward a near-by point.

To determine the rate $\frac{d(\Delta\theta)}{dt}$ at which to servo the heading vector, we derive the following. From Equation (44):

$$\tan\Delta\theta \ = \ \frac{s}{h_c}\tan\phi.$$

Taking the derivative with respect to time:

$$\frac{1}{\cos^2(\Delta\theta)}\frac{d(\Delta\theta)}{dt} \ = \ \frac{s}{h_c\cos^2\phi}\dot{\phi}$$

or

$$\frac{d(\Delta\theta)}{dt} \ = \ \frac{s}{h_c}\frac{\cos^2\Delta\theta}{\cos^2\phi}\dot{\phi} \tag{45}$$

Here $\dot{\phi}$ is the optical flow of the tangent point in the ϕ direction. The value $\dot{\phi}$ can be directly measured in the camera, while the value $\Delta\theta$ is computed from Equation (44). The values s and h_c are a priori known constants. Thus the only measurements needed for computing $\dfrac{d(\Delta\theta)}{dt}$ are visual, i.e., they can be extracted from the image.

A final scheme that can be useful for road following is depicted in Figure 21. The goal is to servo the heading vector $\hat{h}$ so as to maintain the vehicle at a constant distance s from the edge of the road. The method here is to consider an imaginary line on the ground which is perpendicular to the heading vector (and to the camera Y-axis) and is at a constant distance d from the vehicle. We measure the angle θ between the X-axis and the vector from the camera to the point of intersection of the imaginary line and the road edge (point I in Figure 21). The distance s from the road edge to the heading vector, measured along the imaginary line, is

$$ s = \frac{d}{\tan\theta}. $$

If the heading vector is servoed so as to maintain the angle θ constant then, because d is a constant, s will also be maintained at a constant value.

Figure 22 shows how this imaginary line can be determined from a tilt angle δ, measured in the camera YZ-plane. From Figure 22:

$$ d = \frac{h_c}{\tan\delta} $$

This equation shows how the value of δ, which can be measured in the image, defines the distance d of the imaginary line.

From Figure 21, we see that the angle θ should always be smaller than the tangent angle θ_T if the road edge is on the left of the vehicle, and greater than θ_T for a road edge on the right. Since θ_T is continuously changing for a non-circular road, we may want to have several imaginary lines at distances $d_1, \cdots, d_n$, and store several corresponding values $\theta_1, \cdots, \theta_n$. These distances correspond to several tilt angles $\delta_1, \cdots, \delta_n$.

This last control approach is the only one in this paper that requires information about the road at points other than the tangent point. We discuss this kind of approach to indicate that the approaches based on the tangent point can be combined with other approaches in developing robust control algorithms.

5. CONCLUSION

This paper has presented a new approach to vision and control for road following. The approach is based on an analysis of the geometric and motion-related relationships and constraints for road following. This analysis builds upon the visual field theory previously developed by the authors. From this initial analysis, we derived visual cues and control approaches for road following.

We showed that, in principle, the only road feature necessary for following curved, convex roads is the position of the tangent point on the road edge and perhaps its optical flow. In practice, larger portions of the road may have to be extracted in order to reliably find the tangent point. We also showed that fast, simple control approaches are possible that directly use measured image quantities.
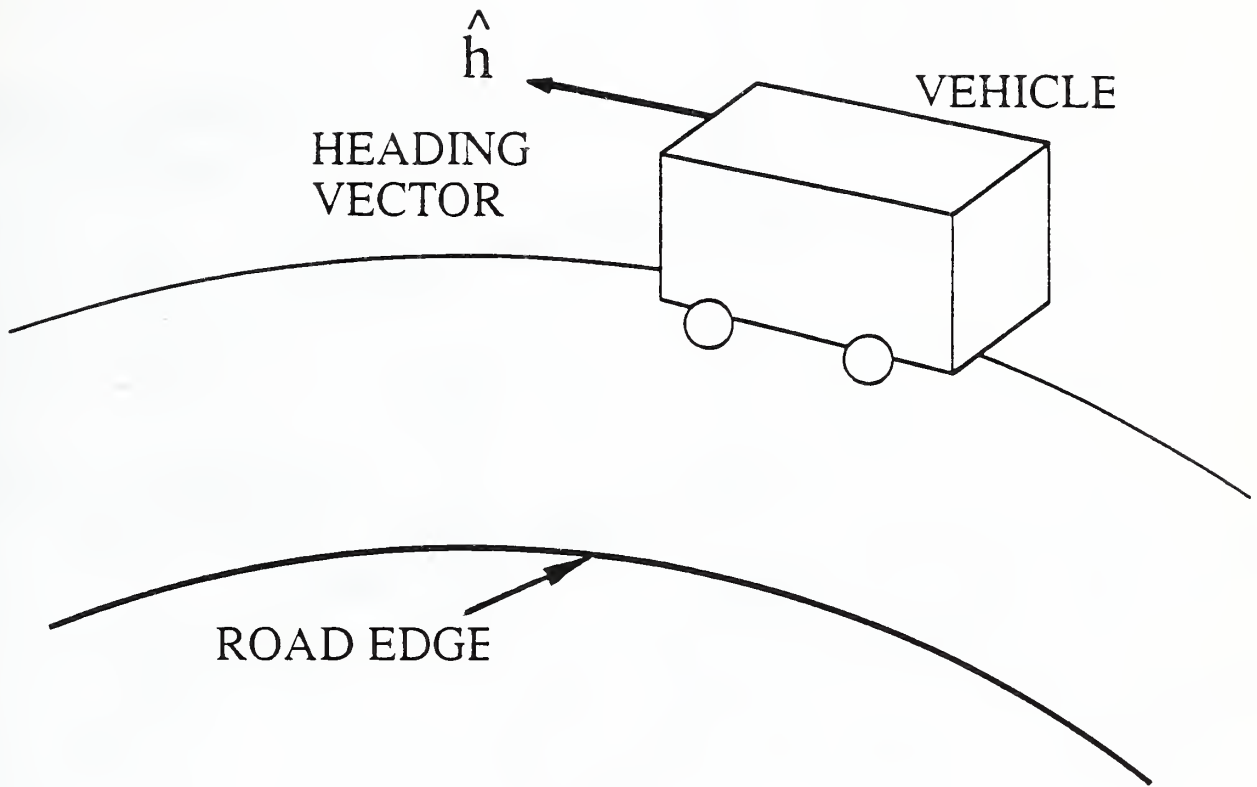
The partial control schemes presented in this paper have not been implemented yet. Current and future work will be directed towards implementing control algorithms that use the approaches suggested in this paper [12]. Issues such as the dynamics of the vehicle, sensitivity, stability, robustness, and timing delays must be considered when developing control algorithms for real vehicles.

Another area for future work is to extend the ideas in this paper to other types of roads. Issues that will need to be addressed include concave roads, roads with two boundaries, where the left and right boundaries are alternatively convex, and roads that are straight (not curved). Of course, to follow real-world roads, the ideas in this paper will have to be integrated with systems that find road edges in real images of highways and city and dirt roads.

REFERENCES

1. Aloimonos, J. "Purposive and Qualitative Active Vision." *Proc. DARPA Image Understanding Workshop,* September 1990.

2. Crisman, J. and Thorpe, C. "Color Vision for Road Following." *Vision and Navigation: The Carnegie Mellon Navlab.* Kluwer Academic Publishers, 1990, Chapter 2.

3. Dickmans, E. and Grafe, V. "Applications of Dynamic Monocular Machine Vision." *Machine Vision and Applications,* Vol. 1, 1988.

4. Dickmans, E. and Grafe, V. "Dynamic Monocular Machine Vision." *Machine Vision and Applications,* Vol. 1, 1988.

5. Horn, B.K.P. *Robot Vision,* MIT Press, 1986.

6. Meriam, J.L. *Dynamics,* John-Wiley & Sons, 1975.

7. Raviv, D. "A Quantitative Approach to Camera Fixation." Internal Report NIS-TIR 4324, National Institute of Standards and Technology, May 1990.

8. Raviv, D. and Herman, M. "Towards an Understanding of Camera Fixation." *Proc. 1990 IEEE International Conference on Robotics and Automation,* Cincinnati, Ohio, May 1990, 28-33.

9. Thorpe, C., Hebert, M., Kanade, T. and Shafer, S. "Vision and Navigation for the Carnegie-Mellon Navlab." *IEEE Trans. on Pattern Analysis and Machine Intelligence,* 10(3), 1988.

10. Turk, M., Morgenthaler, D., Gremban, K. and Marra, M. "VITS -- A Vision System for Autonomous Land Vehicle Navigation." *IEEE Trans. on Pattern Analysis and Machine Intelligence,* May 1988.

11. Waxman, A., LeMoigne, J., Davis, L. and Siddalingalah, T. "A Visual Navigation System for Autonomous Land Vehicle." *IEEE Journal Robotics and Automation,* RA-3:124-141, April 1987.

12. Yakali, H. H., Raviv, D. and Herman, M. "A New Concept for Road Tracking: Imaginary Circular Roads." In preparation.

HEADING
VECTOR

$\hat{h}$

VEHICLE

ROAD EDGE

1 (a)

Figure 1: Road Following. (a) 3-D (b) Top View

$\hat{h}$

A POINT ON THE
VEHICLE

A

S

TANGENT TO LOCAL
CURVATURE

B

ROAD EDGE

O

1(b)
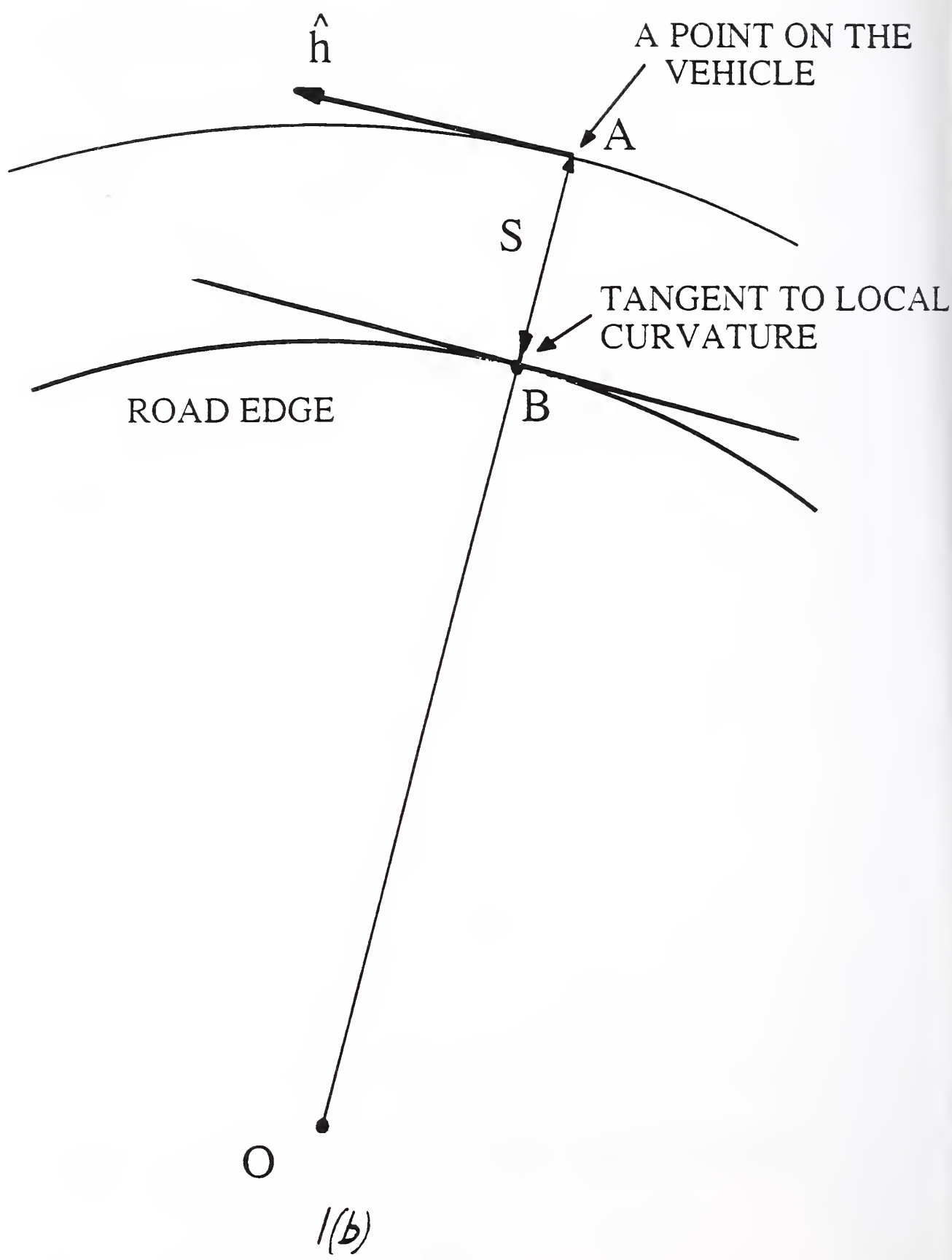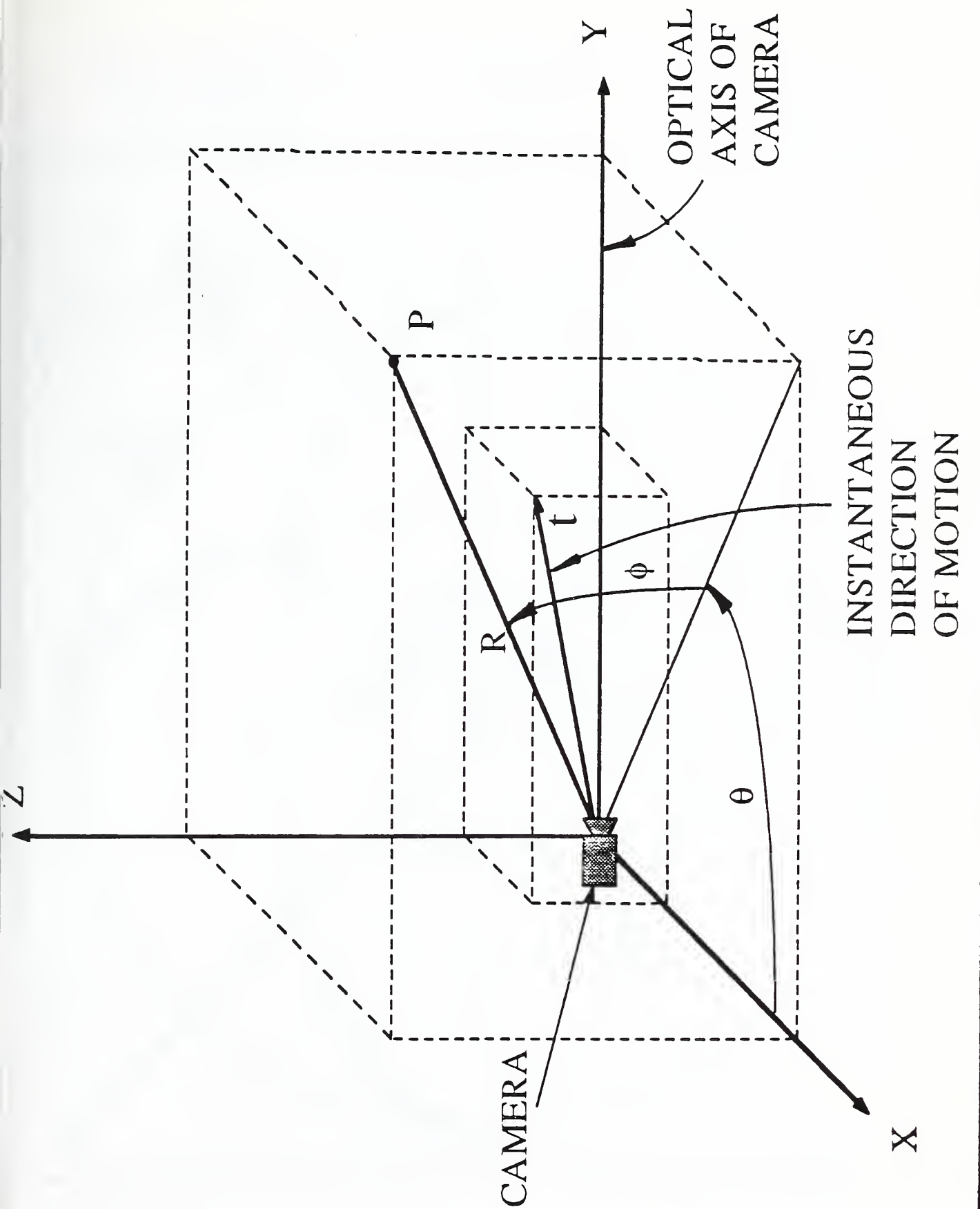
Figure 2: Coordinate System Fixed to Camera

21
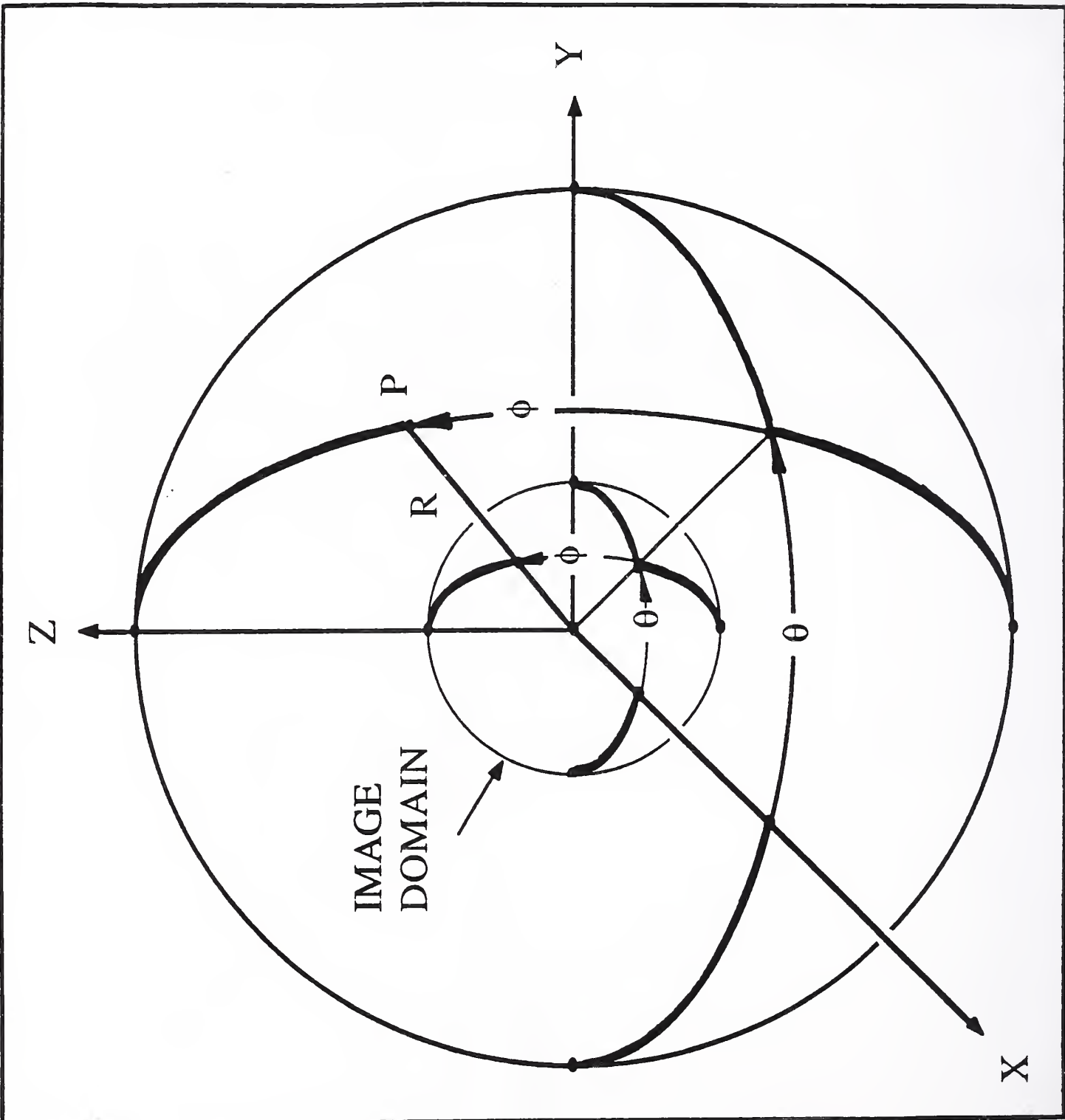
Figure 3: Image Domain
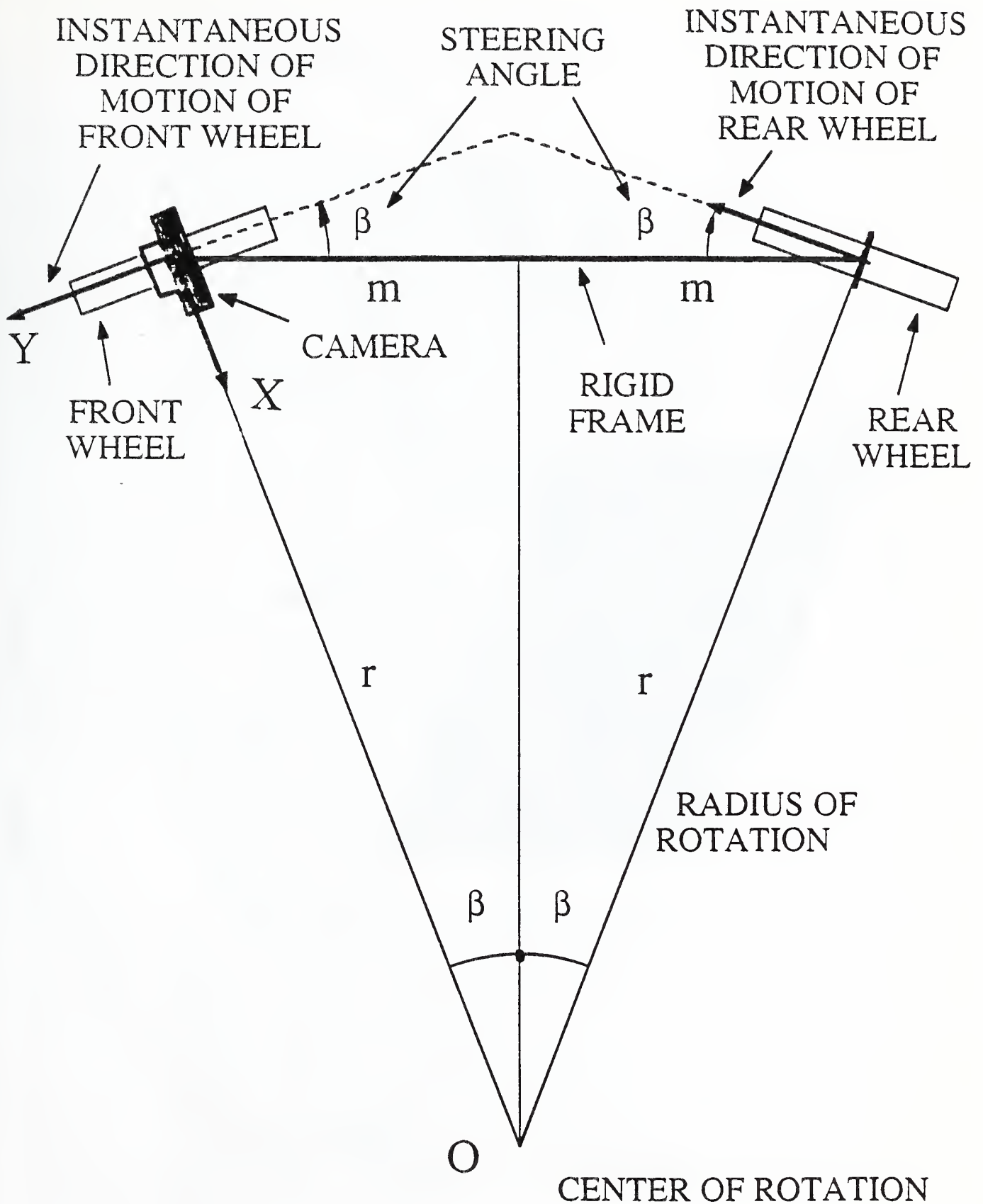
Figure 4: Two Wheel Vehicle with Camera

23
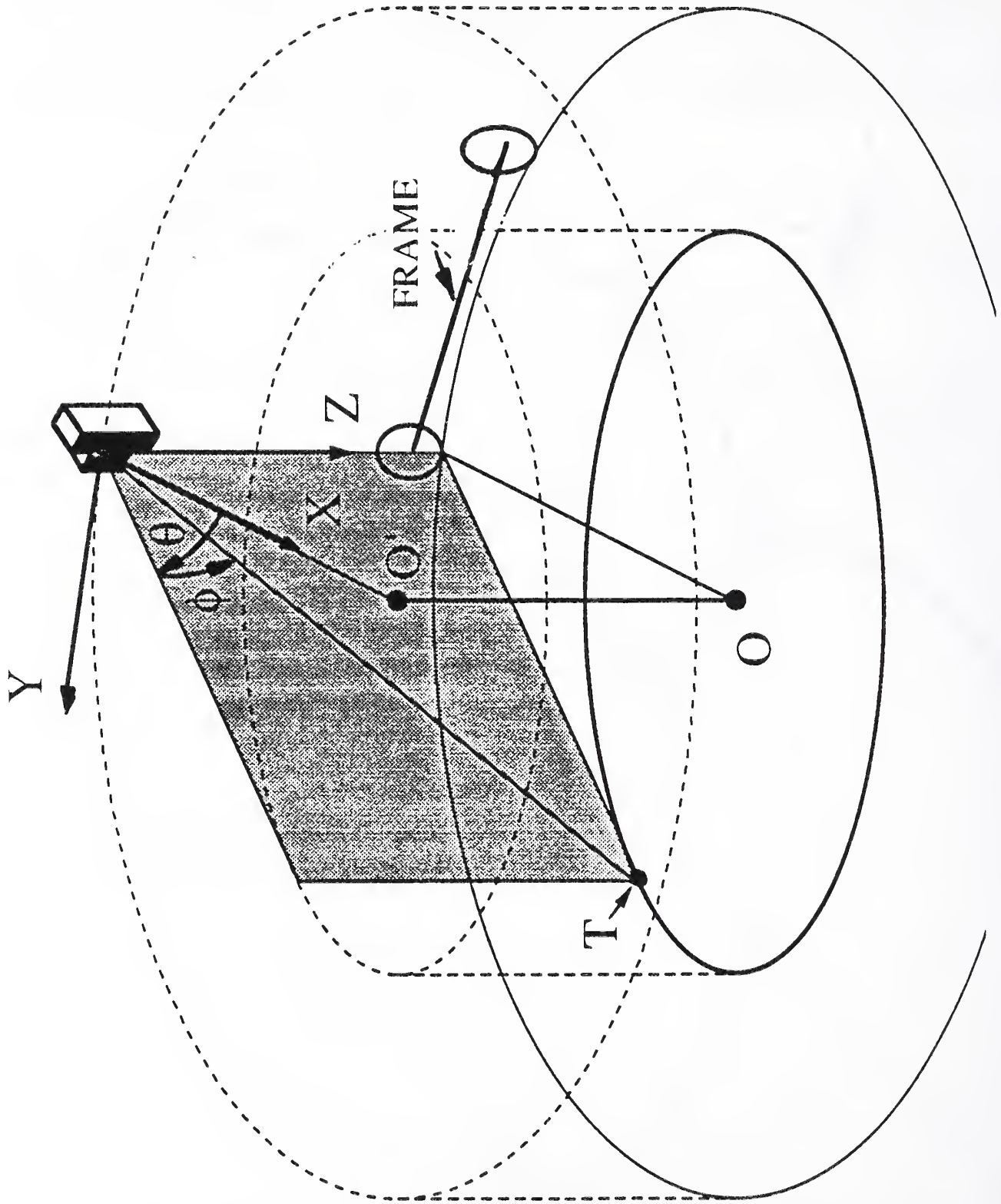
Figure 5: Overall Description of System

24

Figure 6: Top View

25
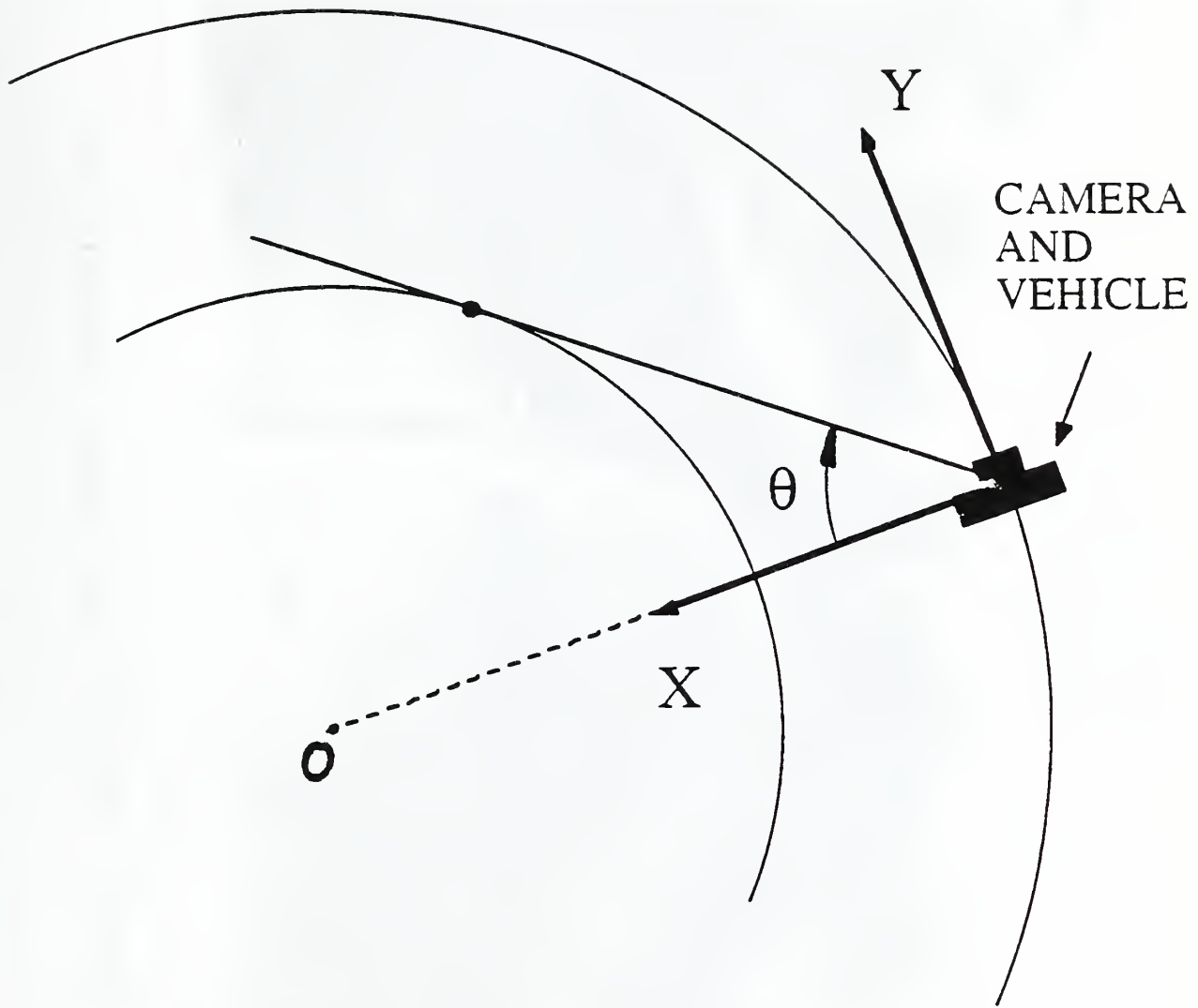
Figure 7: Image Obtained from Camera Mounted on a Vehicle
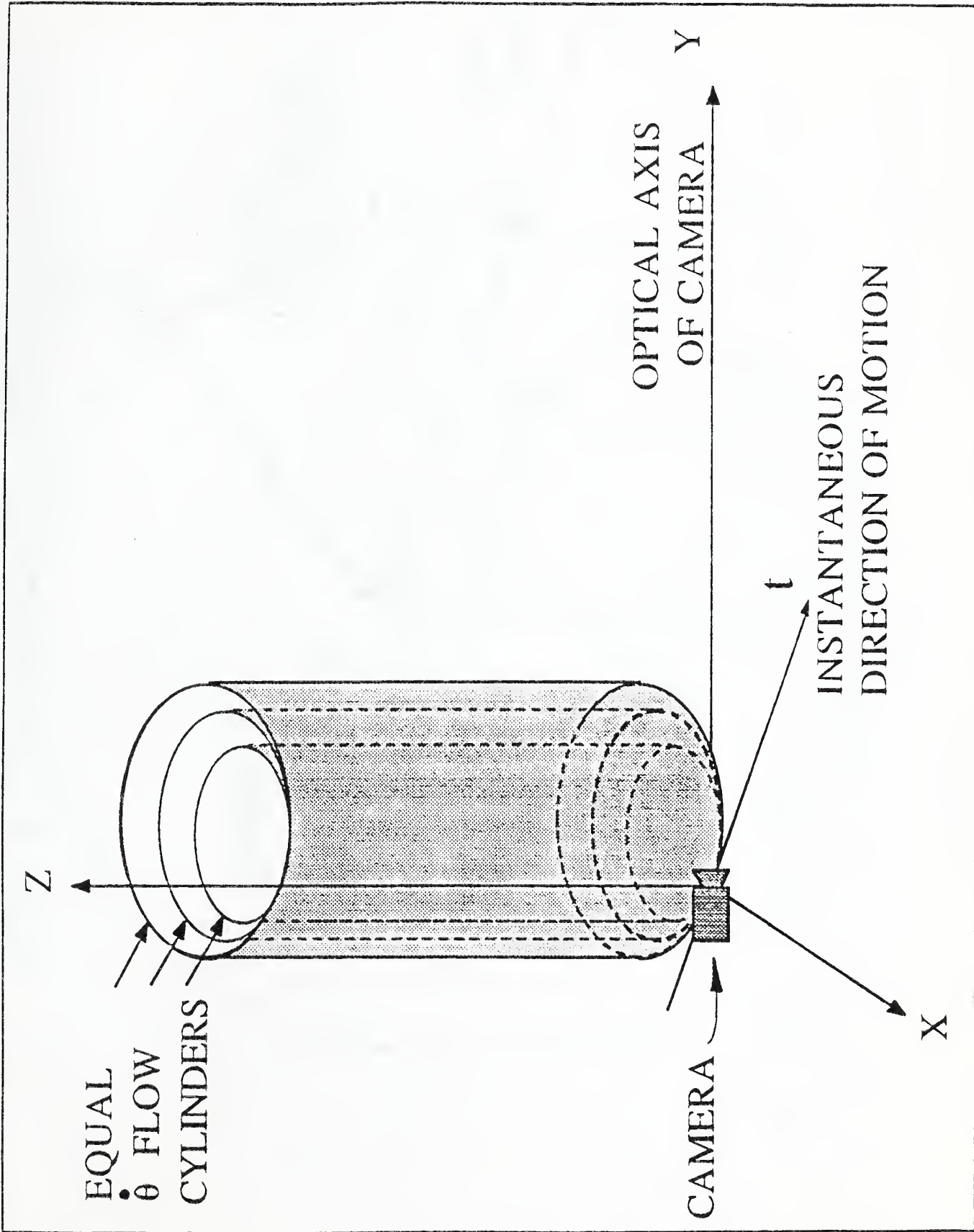
Figure 8: Equal $\dot{\theta}$ Flow Cylinders

27

$$\left(\frac{-V}{2(C+\dot{\theta})}, \frac{U}{2(C+\dot{\theta})}, 0\right)$$

$$\left(\frac{-V}{C+\dot{\theta}}, \frac{U}{C+\dot{\theta}}, 0\right)$$

Z

Y

OPTICAL
AXIS

t

INSTANTANEOUS
DIRECTION OF
MOTION

X

CIRCLE
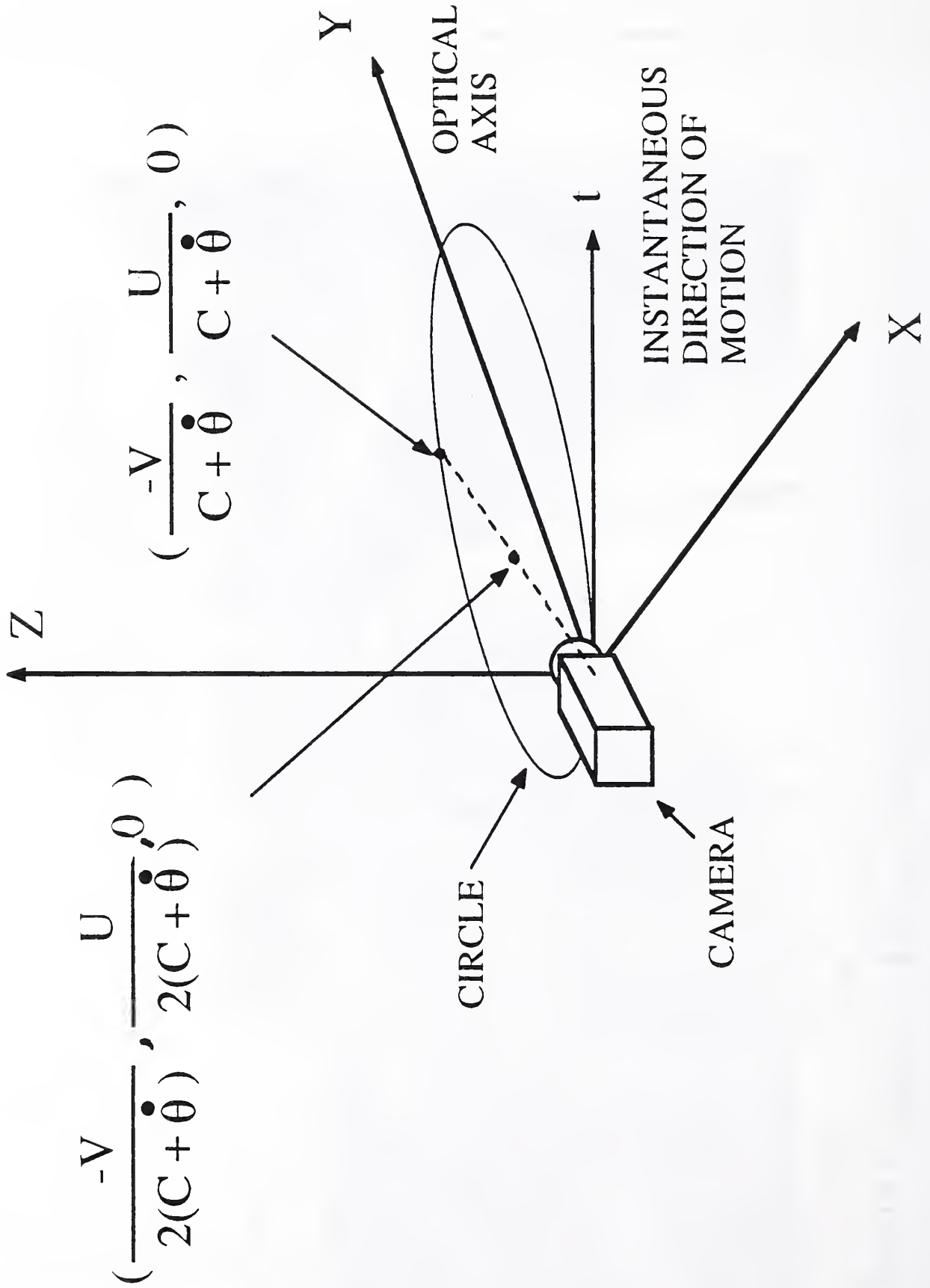
CAMERA

Figure 9: Section of a Zero Flow Cylinder
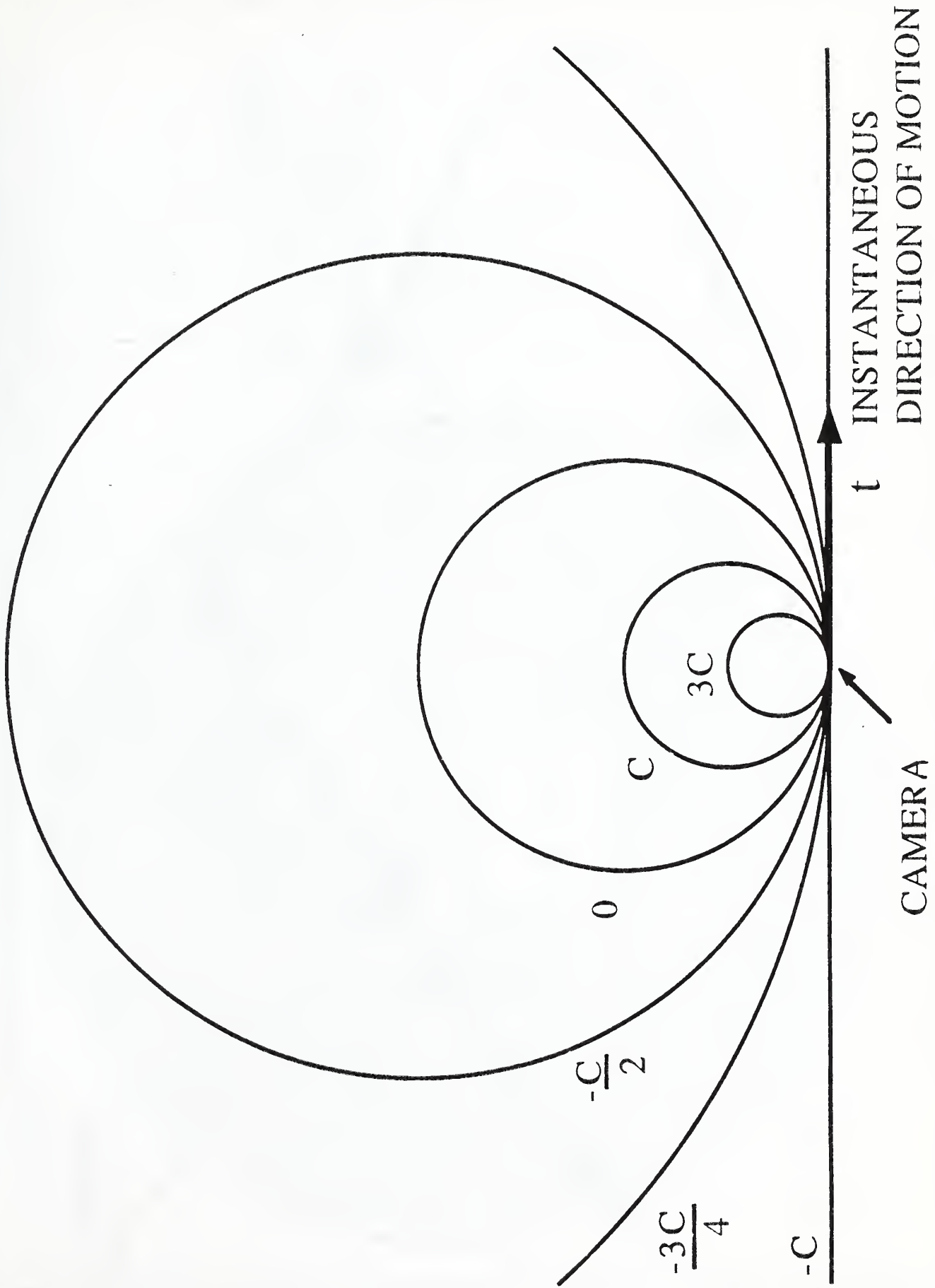
Figure 10: Optical Flow Values Due To Camera Motion
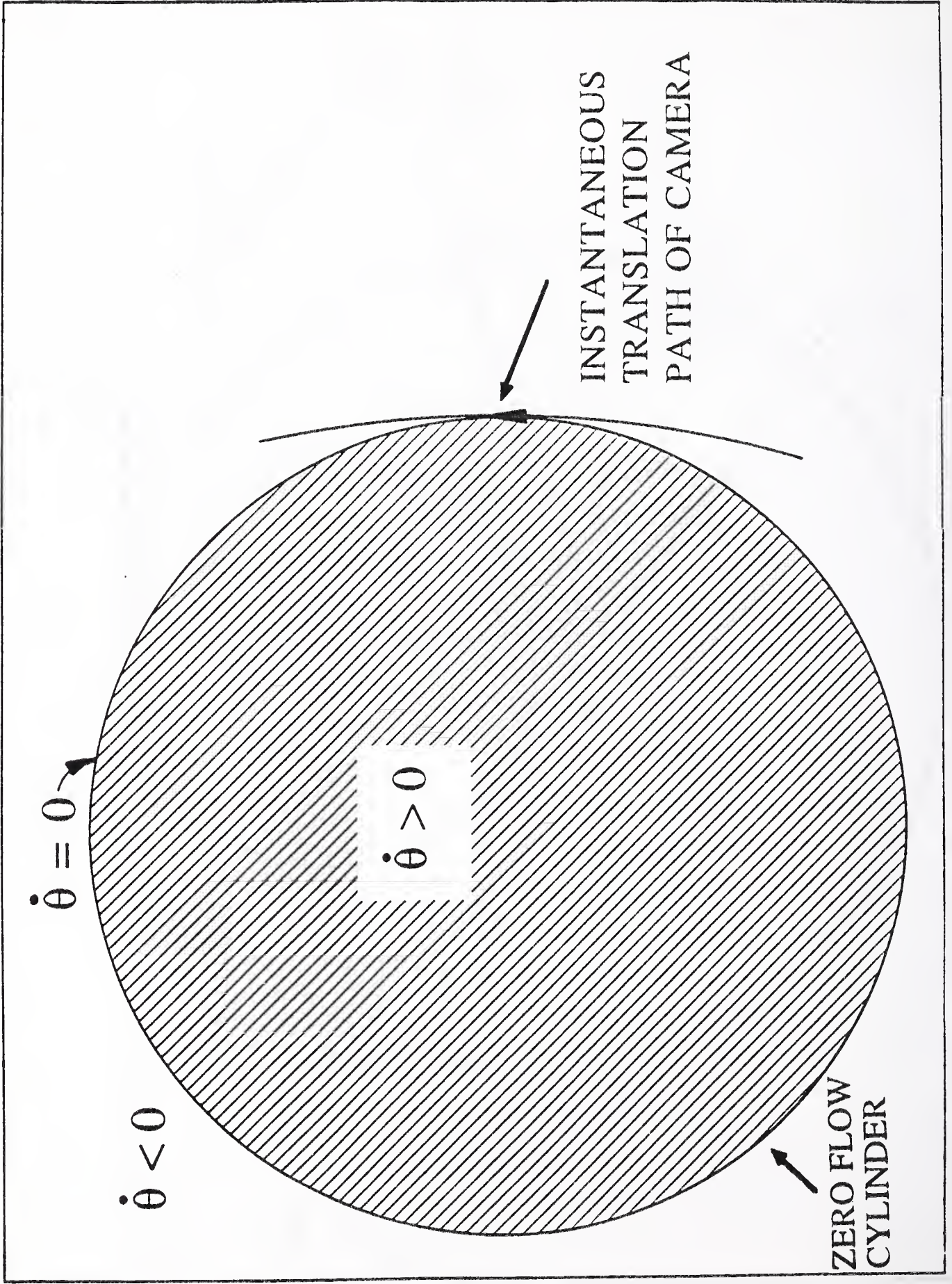
Figure 11: Section of Zero Flow Cylinder
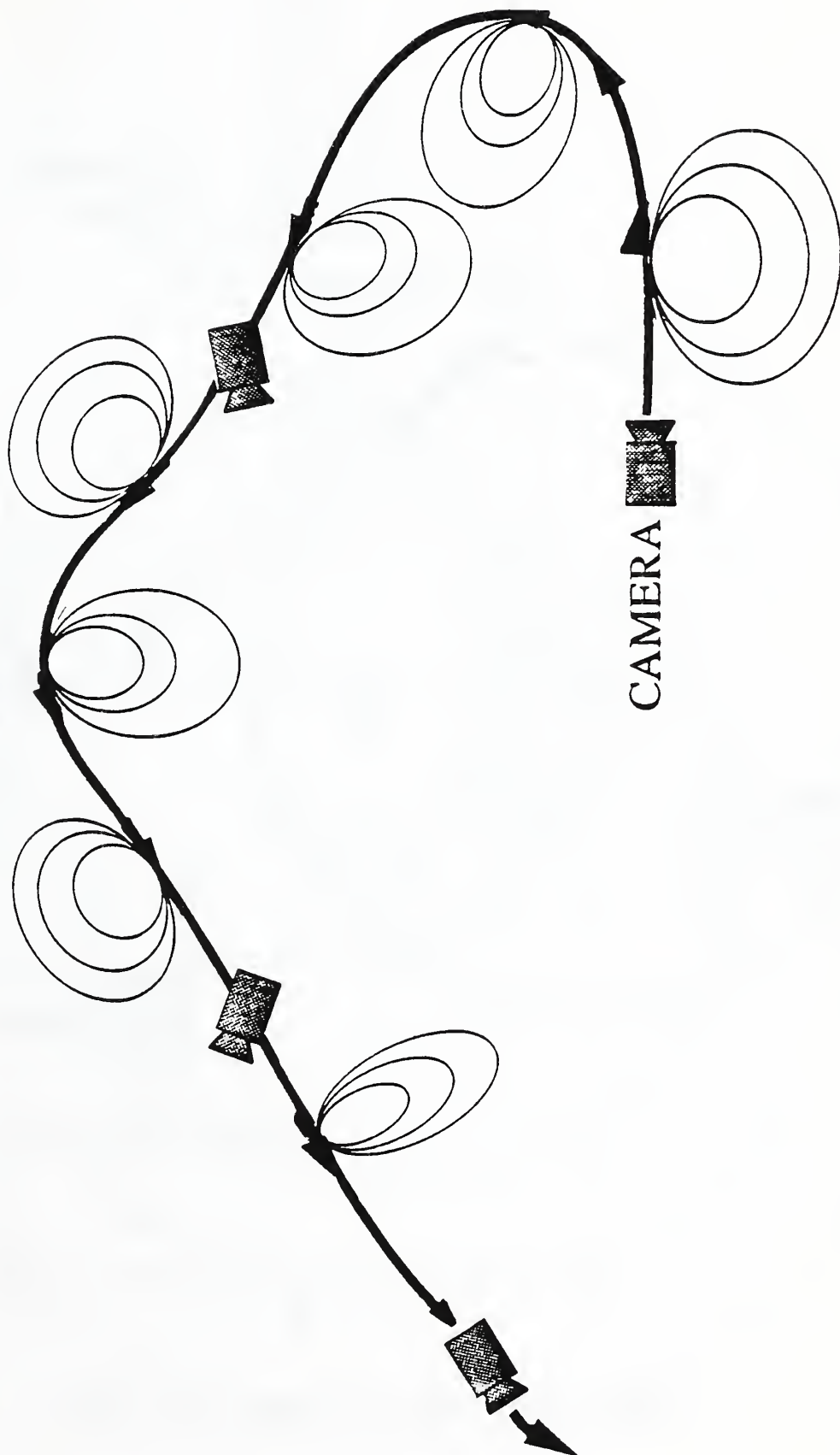
Figure 12: Section of Zero Flow Cylinder as a Function of Time

CAMERA
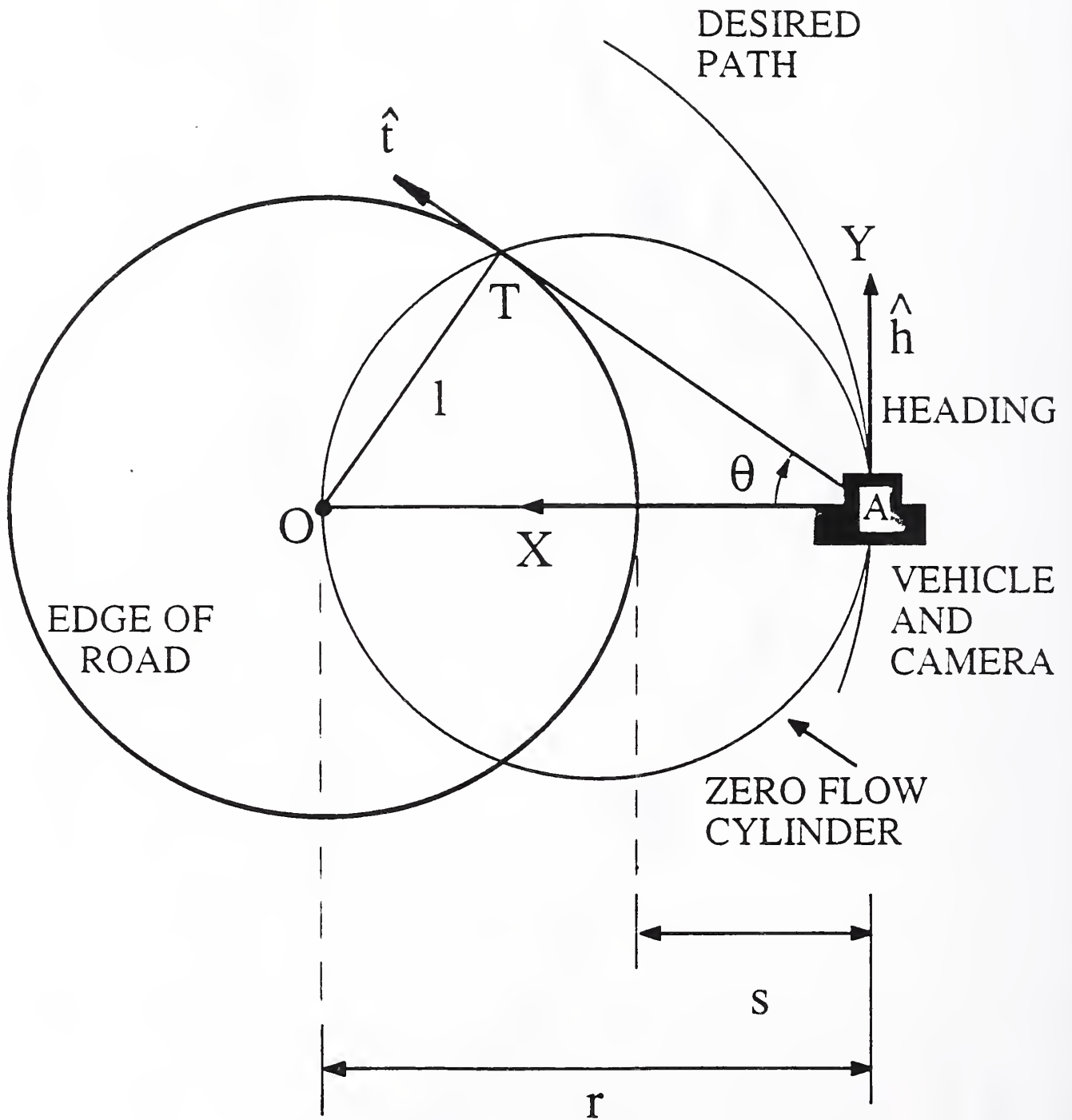
Figure 13: Circular Edge: Top View
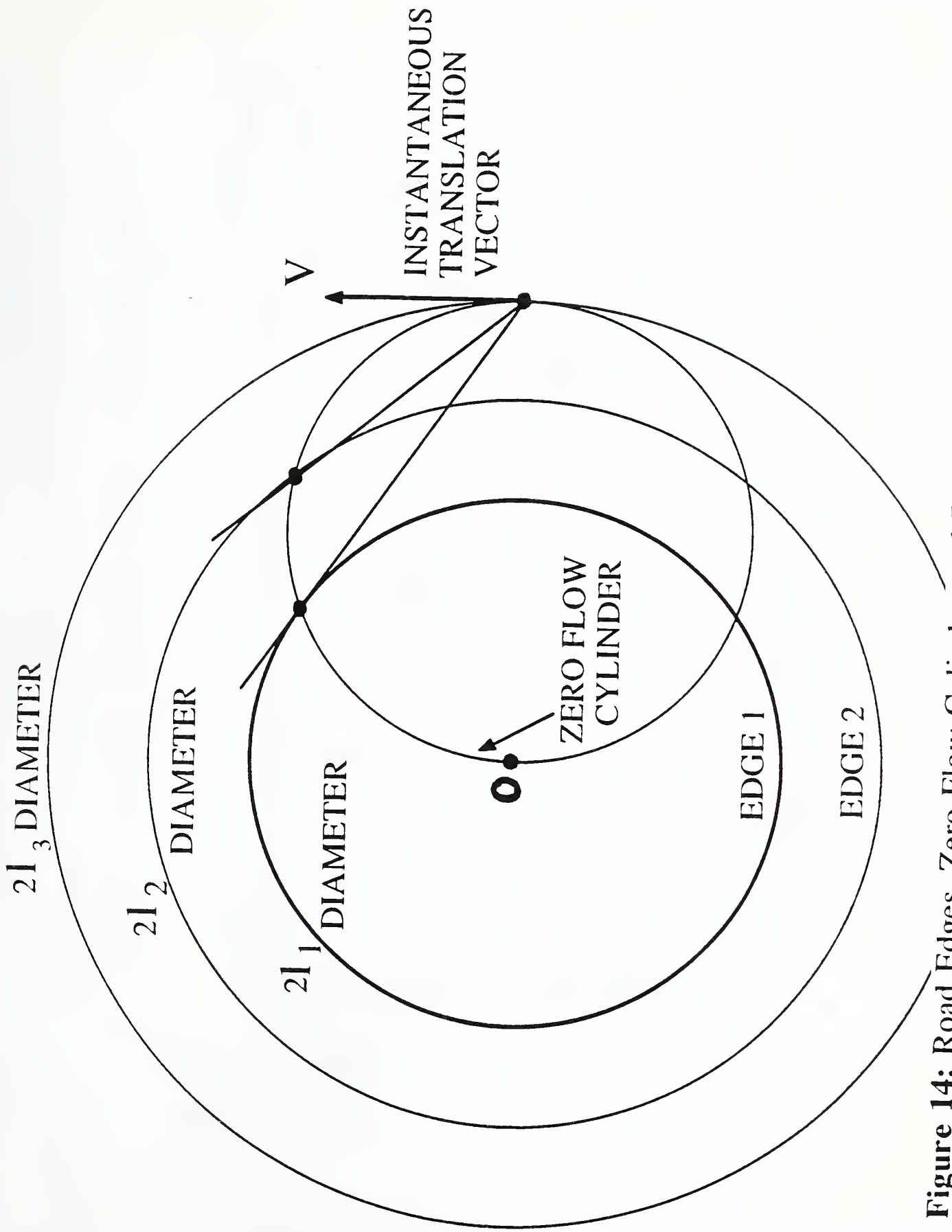
Figure 14: Road Edges, Zero Flow Cylinder, and Tangent Points
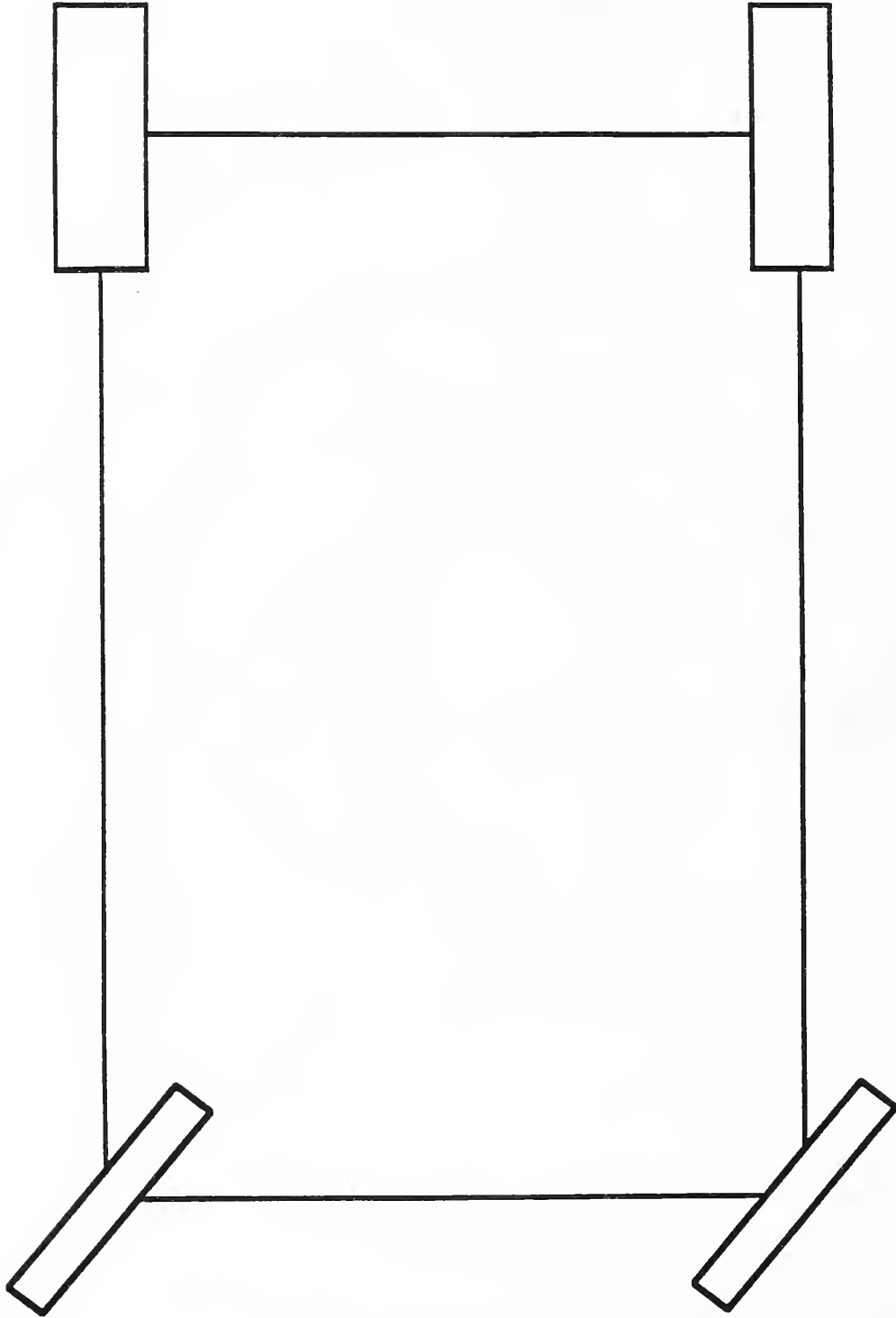
Figure 15: Four Wheeled Vehicle with Front Wheel Steering
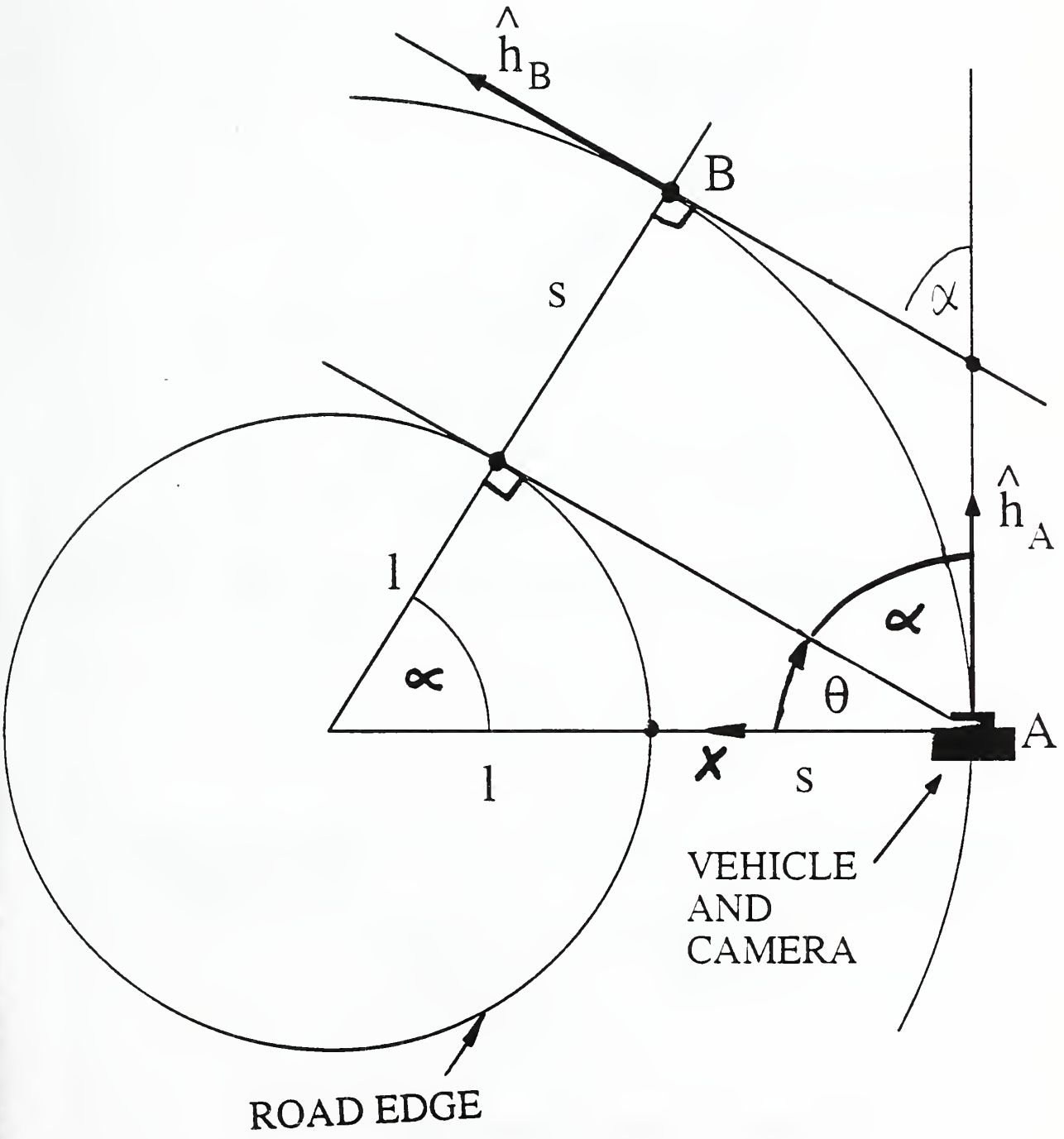
Figure 16: Turning Rate Analysis
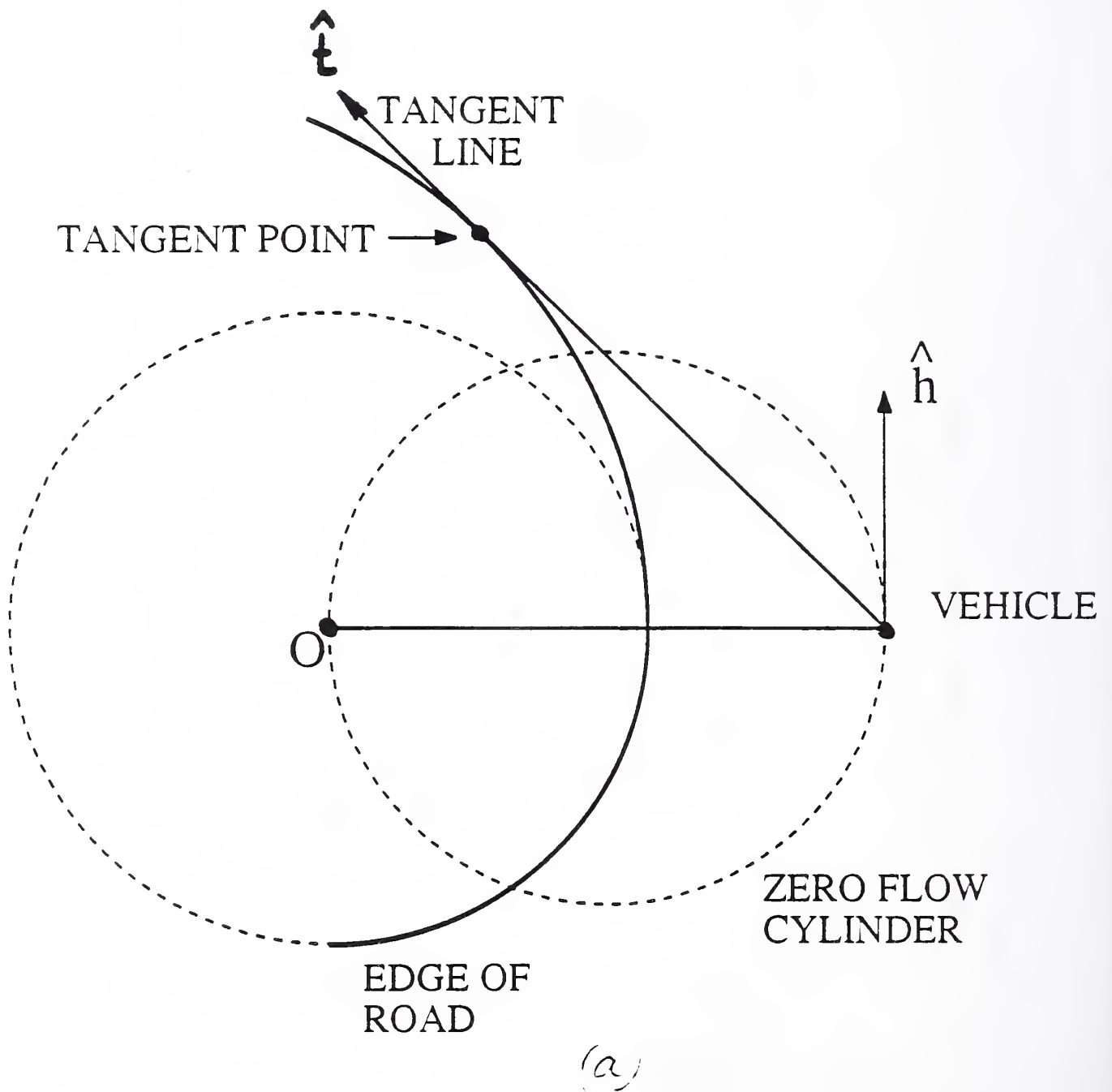
Figure 17: Road Following:
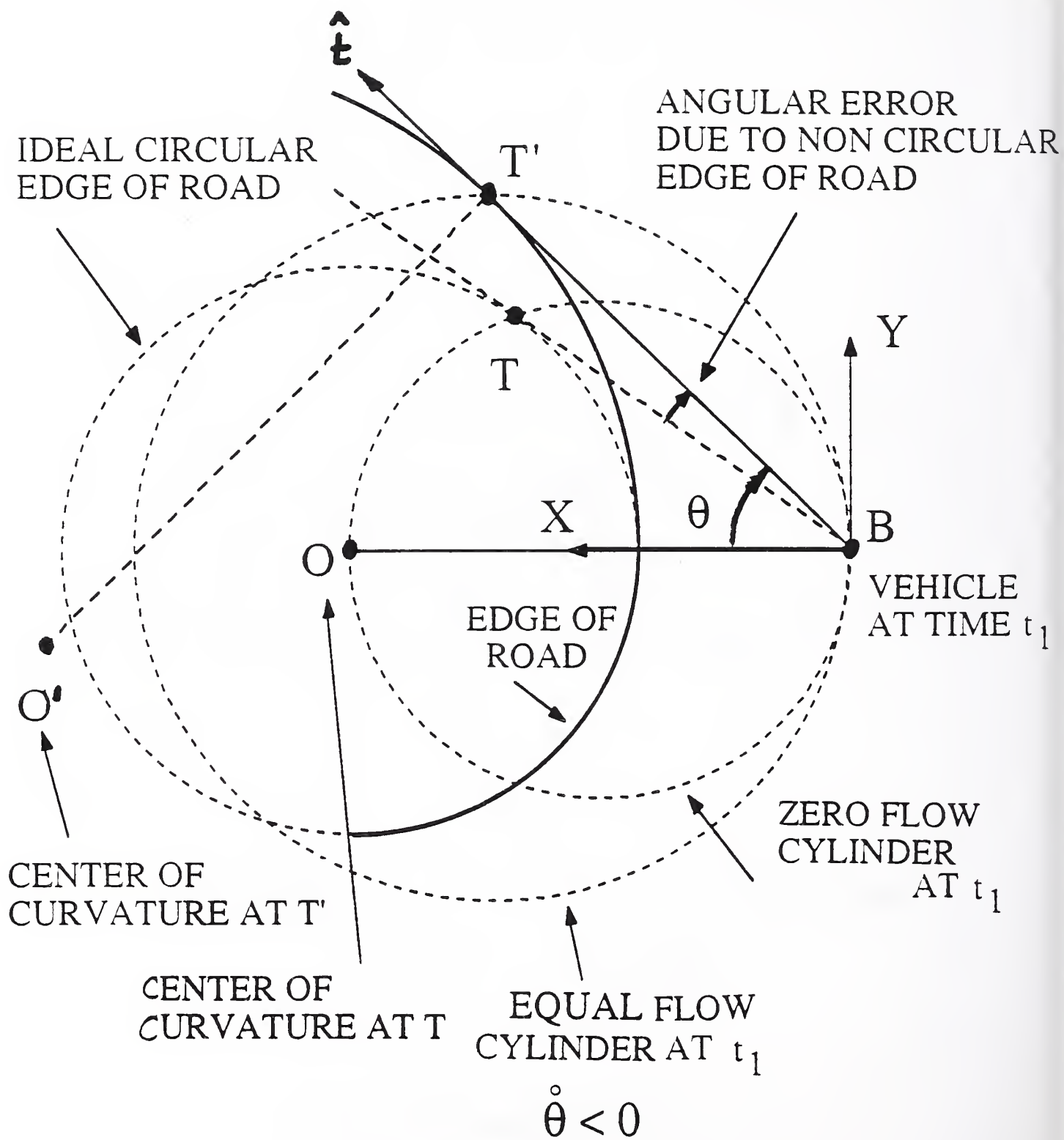 (a) Increasing Radius of Curvature
  (b) Decreasing Radius of Curvature

$\hat{t}$

TANGENT
POINT

TANGENT
LINE

$\hat{h}$

VEHICLE

O

ZERO FLOW
CYLINDER

EDGE OF
ROAD
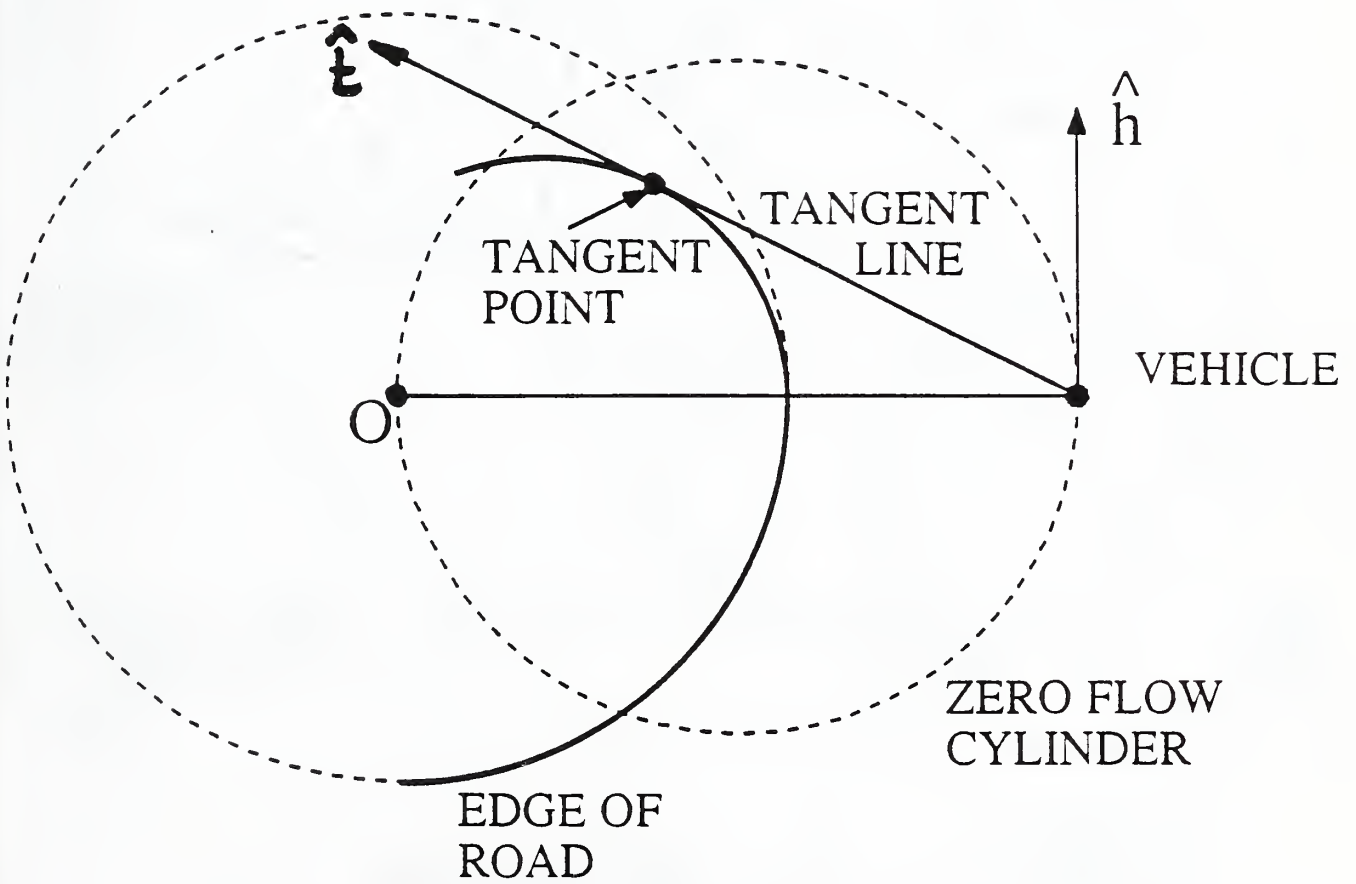
17 (b)

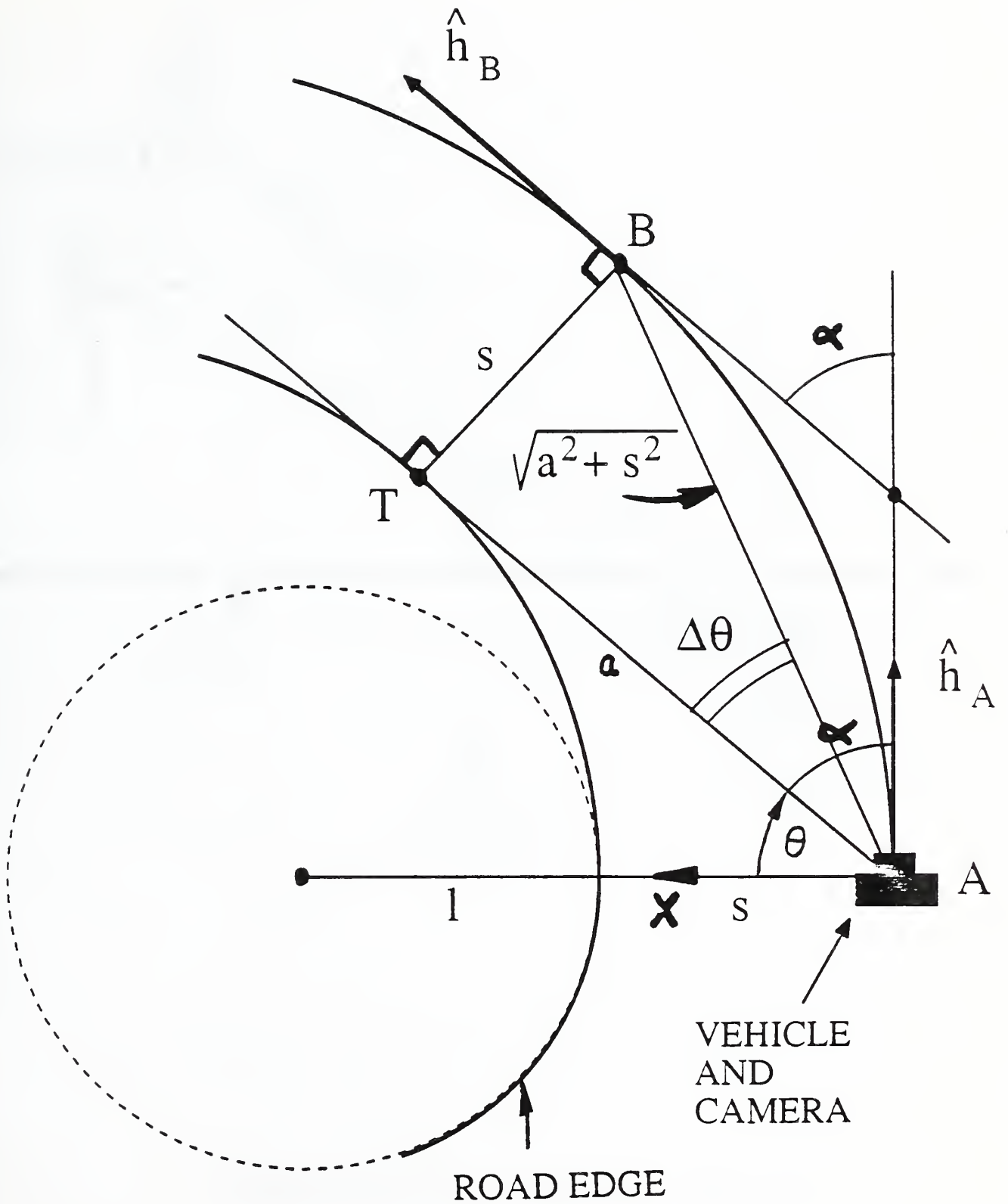**Figure 18:** Change in Curvature: Analysis

Figure 19: Road Following - Analysis
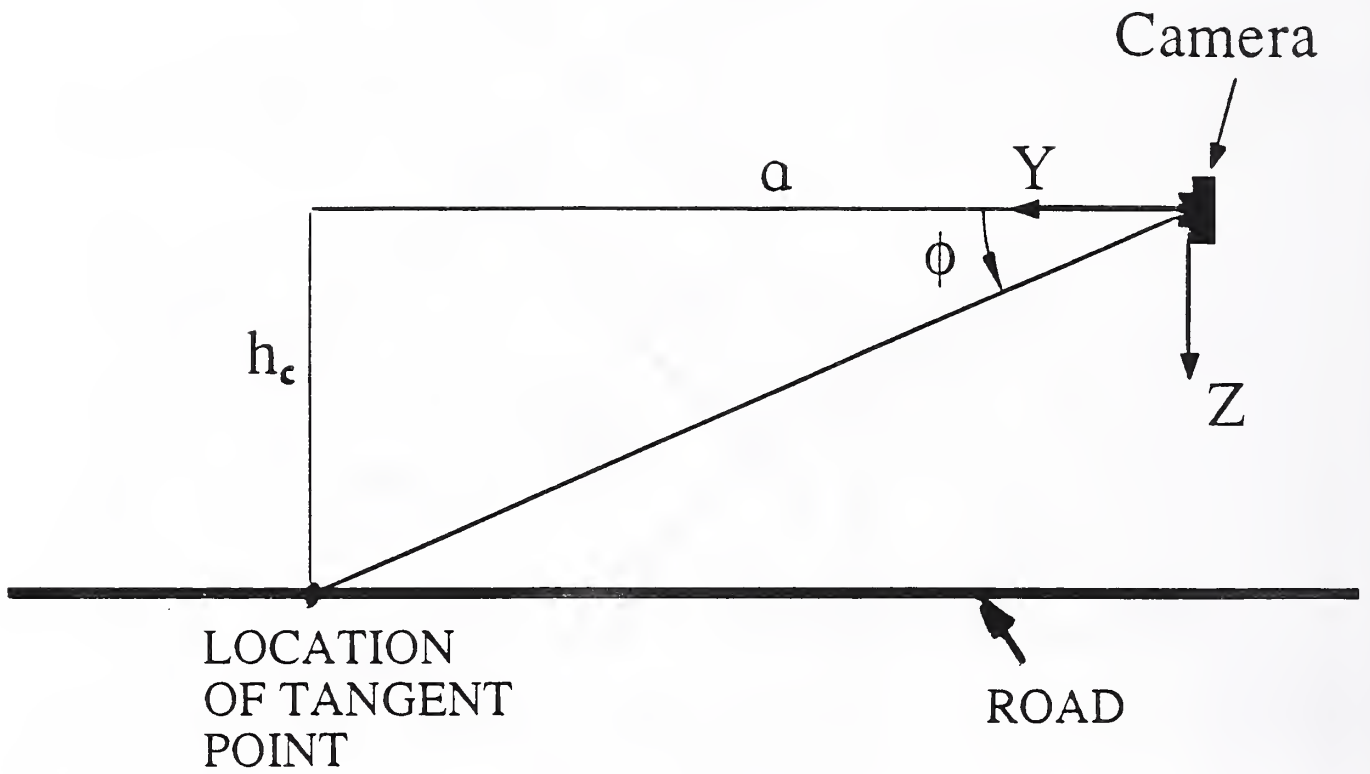
Figure 20: Road Following - Analysis
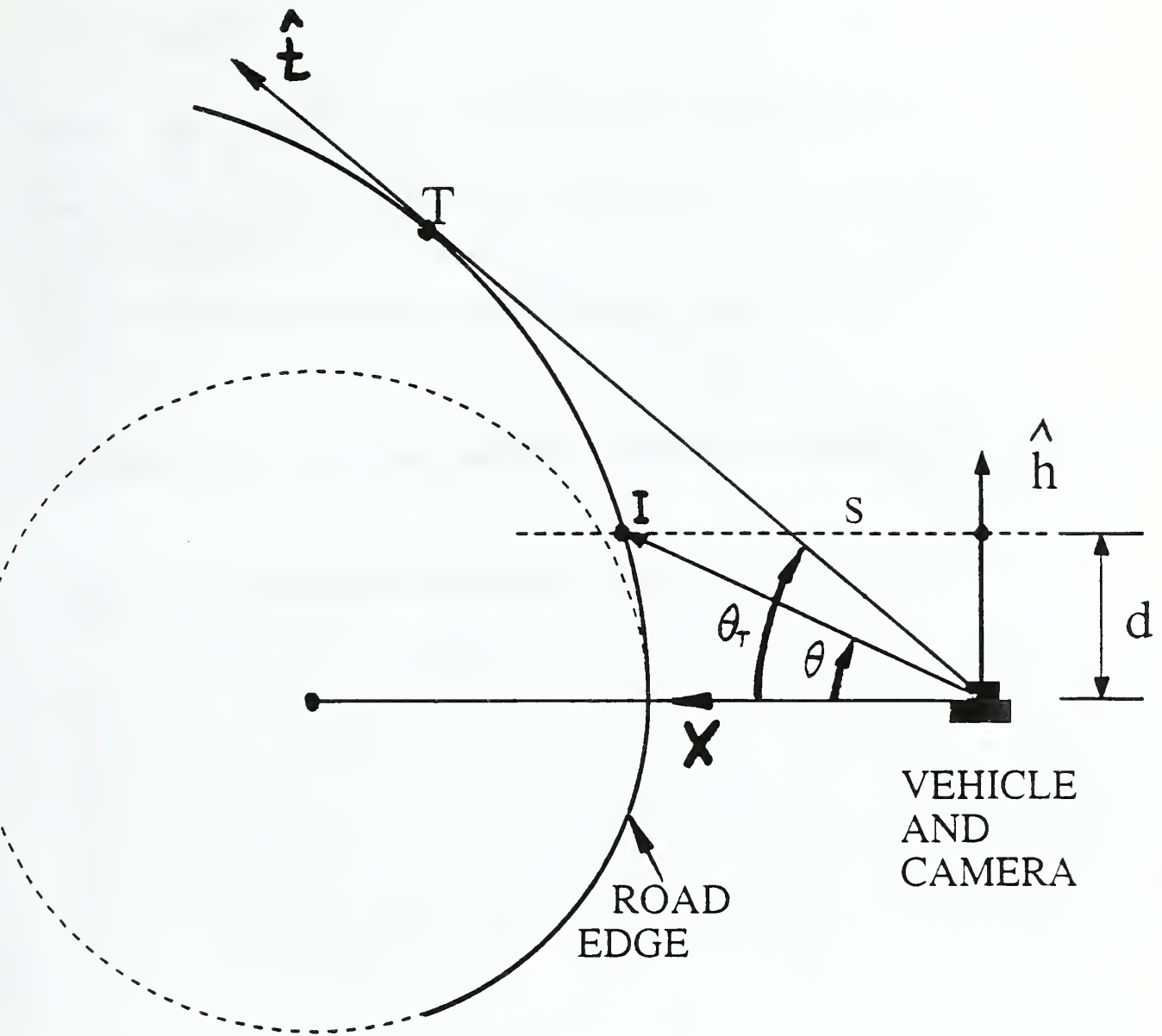
Figure 21: Road Following - Analysis

41

Figure 22: Road Following - Analysis
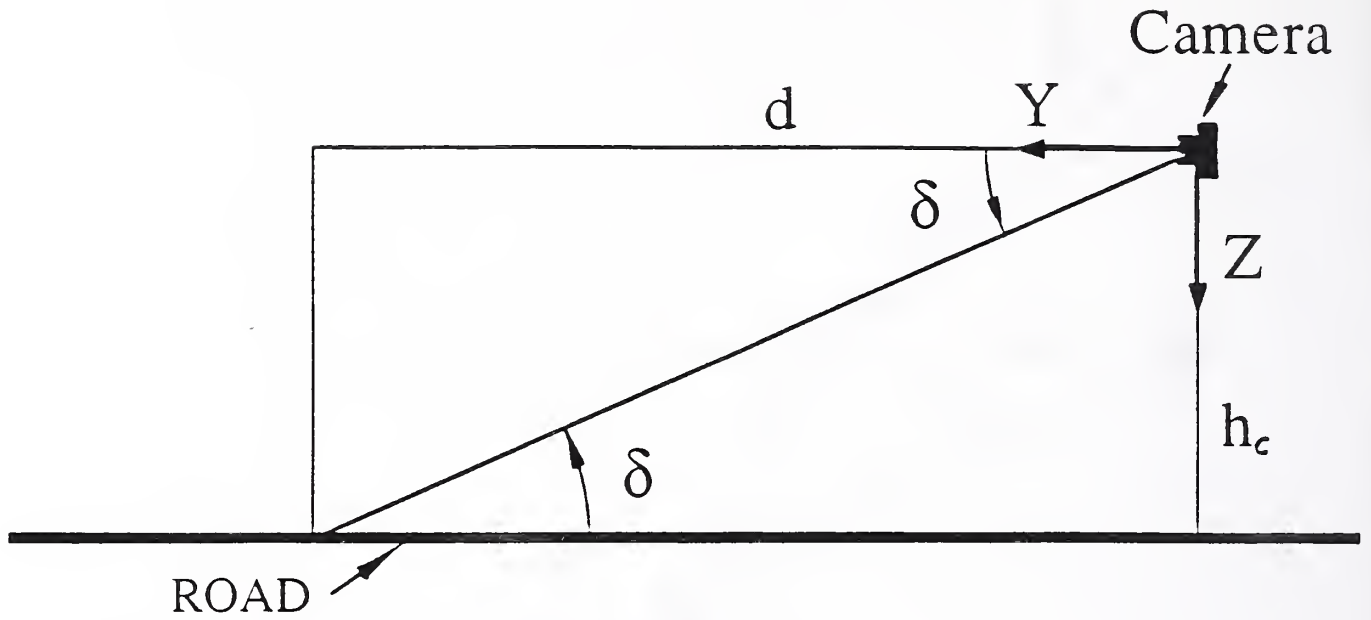
U.S. DEPARTMENT OF COMMERCE
NATIONAL INSTITUTE OF STANDARDS AND TECHNOLOGY

BIBLIOGRAPHIC DATA SHEET

4. TITLE AND SUBTITLE

A New Approach to Vision and Control for Road Following

5. AUTHOR(S)

Daniel Raviv and Martin Herman

6. PERFORMING ORGANIZATION (IF JOINT OR OTHER THAN NIST, SEE INSTRUCTIONS)

U.S. DEPARTMENT OF COMMERCE
NATIONAL INSTITUTE OF STANDARDS AND TECHNOLOGY
GAITHERSBURG, MD 20899

7. CONTRACT/GRANT NUMBER

8. TYPE OF REPORT AND PERIOD COVERED

9. SPONSORING ORGANIZATION NAME AND COMPLETE ADDRESS (STREET, CITY, STATE, ZIP)

10. SUPPLEMENTARY NOTES

11. ABSTRACT (A 200-WORD OR LESS FACTUAL SUMMARY OF MOST SIGNIFICANT INFORMATION. IF DOCUMENT INCLUDES A SIGNIFICANT BIBLIOGRAPHY OR LITERATURE SURVEY, MENTION IT HERE.)

This paper deals with a new quantitative, vision-based approach to road following. It is based on the theoretical framework of the recently developed optical flow-based visual field theory. By building on this theory, we suggest that motion commands can be generated directly from a visual feature, or cue, consisting of the projection into the image of the tangent point to the edge of the road, along with the optical flow of this point. Using this cue, we suggest several different vision-based control approaches. There are several advantages to using this visual cue: (1) it is extracted directly from the image, i.e., there is no need to reconstruct the scene, (2) for many road following situations this is the only necessary visual cue, (3) only the horizontal component of the optical flow of the tangent point needs to be extracted, (4) it has a scientific basis, i.e., the described techniques are not ad-hoc, (5) the related computations are relatively simple and thus suitable for real-time applications. For each control approach, we derive the value of the related steering commands.

12. KEY WORDS (6 TO 12 ENTRIES; ALPHABETICAL ORDER; CAPITALIZE ONLY PROPER NAMES; AND SEPARATE KEY WORDS BY SEMICOLONS)

autonomous vehicles; mobile robots; optical flow; road following; robot control; robot vision

13. AVAILABILITY

X	UNLIMITED
	FOR OFFICIAL DISTRIBUTION. DO NOT RELEASE TO NATIONAL TECHNICAL INFORMATION SERVICE (NTIS).
	ORDER FROM SUPERINTENDENT OF DOCUMENTS, U.S. GOVERNMENT PRINTING OFFICE, WASHINGTON, DC 20402.
X	ORDER FROM NATIONAL TECHNICAL INFORMATION SERVICE (NTIS), SPRINGFIELD, VA 22161.

14. NUMBER OF PRINTED PAGES

45

15. PRICE

A03

ELECTRONIC FORM